

Manuscript Number: JBIOTEC-D-20-00840R1

Title: An NADH preferring acetoacetyl-CoA reductase is engaged in poly-3-hydroxybutyrate accumulation in Escherichia coli

Article Type: Research Paper

Section/Category: Physiology/Biochemistry

Keywords: acetoacetyl-CoA reductase; NADH; NADPH; oxygen limitation; cofactor specificity; Polyhydroxybutyrate

Corresponding Author: Mr. Karel Olavarria, Ph.D.

Corresponding Author's Institution:

First Author: Karel Olavarria, Ph.D.

Order of Authors: Karel Olavarria, Ph.D.; Alexandre Carnet; Joachim van Ranselaar; Caspar Quakkelaar; Ricardo Cabrera; Leonor Guedes da Silva; Aron L Smids; Pablo Villalobos; Mark CM van Loosdrecht; Sebastian Aljoscha Wahl

Abstract: Oxygen supply implies higher production cost and reduction of maximum theoretical yields. Thus, generation of fermentation products is more cost-effective. Aiming to find a key piece for the production of (poly)-3-hydroxybutyrate (PHB) as a fermentation product, here we characterize an acetoacetyl-CoA reductase, isolated from a Candidatus Accumulibacter phosphatis-enriched mixed culture, showing a  $(k_{cat}NADH/KMNADH)/(k_{cat}NADPH/KMNADPH) > 500$ . Further kinetic analyses indicate that, at physiological concentrations, this enzyme clearly prefers NADH, presenting the strongest NADH preference so far observed among the acetoacetyl-CoA reductases. Structural and kinetic analyses indicate that residues between E37 and P41 have an important role for the observed NADH preference. Moreover, an operon was assembled combining the phaCA genes from Cupriavidus necator and the gene encoding for this NADH-preferring acetoacetyl-CoA reductase. Escherichia coli cells expressing that assembled operon showed continuous accumulation of PHB under oxygen limiting conditions and PHB titer increased when decreasing the specific oxygen consumption rate. Taken together, these results show that it is possible to generate PHB as a fermentation product in E. coli, opening opportunities for further protein/metabolic engineering strategies envisioning a more efficient anaerobic production of PHB.

Research Data Related to this Submission

-----  
Title: NADH-driven polyhydroxybutyrate accumulation in E. coli dataset 2  
Repository: Mendeley Data  
<http://dx.doi.org/10.17632/954dxdncrv.1>

Delft, October 15<sup>th</sup>, 2020

Subject: Submission revised manuscript JBIOTEC-D-20-00840

Dear professor Christoph W. Sensen,  
Chief Editor Journal of Biotechnology

We would like to thank the Editor for the opportunity to reconsider for publication our manuscript “An NADH-preferring acetoacetyl-CoA reductase enables the generation of poly(3-hydroxybutyrate) as a fermentation product in *Escherichia coli*”. In this Cover Letter, we would like to highlight some changes in the revised version.

First, following the suggestion of one of the reviewers, we changed the manuscript’s title. The new title is “An NADH preferring acetoacetyl-CoA reductase is engaged in poly-3-hydroxybutyrate accumulation in *Escherichia coli*”.

Following the suggestion of another reviewer, in the revised version we eliminated the analyses focused in the identification of kinetic and bioenergetic bottlenecks. Instead, we prepared another article where we are showing some data and modelling analyses with more details. This second article will be submitted to Data in Brief. However, the information contained in that second paper is **not** necessary to understand and follow the ideas we are proposing in this manuscript.

To facilitate the reproduction of our results, data and scripts employed in this manuscript are now freely available as a [repository](#) in Mendeley data.

Overall, some parts of the original document were suppressed/modified/extended to answer the questions raised by the reviewers. To facilitate the localization of these answers in the revised manuscript, we are citing these new fragments in the document “Answers to Reviewers”.

We hope this revised version satisfy the concerns raised by the reviewers and be considered for publication in the Journal of Biotechnology.

Best regards,

Karel Olavarria Gamez and Aljoscha Wahl, on behalf of the collective of authors

## Answer to Reviewers

We would like to thank the reviewers for the constructive comments on our manuscript. As a result of the revision, some parts of the originally submitted manuscript were modified. To facilitate the localization of the modified parts, we are citing in some cases the new text resulting from the correction.

Best regards,

Karel Olavarria Gamez and Aljoscha Wahl, on behalf of the collective of authors

### Reviewer#1:

This article by Olavarria and co-workers describes the identification and characterization of an NADH-preferring acetoacetyl-CoA reductase (AAR) from the bacterium *Candidatus Accumulibacter phosphatis*. Kinetic characterization revealed that this AAR has the highest preference for NADH among the previously characterized AAR homologues. Homology modeling allowed the authors to identify amino acid residues (37 – 41) that likely interact with the cofactor, thereby affecting cofactor specificity. Mutation of these residues in *C. necator* appeared to improve the specificity of the enzyme for NADH over NADPH. The accumulation of PHB in an *E. coli* strain expressing phaCA from *C. necator* and the AAR from *Ca. A. phosphatis* demonstrated that the AAR is functional in vivo, and participates in PHB accumulation, which increases under oxygen limitation. Lastly, flux balance analyses identified potential bottlenecks in the pathway that will need to be alleviated to achieve higher PHB accumulation in *E. coli*. Overall, I found the findings in this work interesting and insightful. I think that the advances detailed here will help guide future efforts to engineer microorganisms for PHB accumulation.

However, some of the results were not fully explained/discussed in the text, which seemed like a missed opportunity for the authors to emphasize their findings.

In addition, the exciting results of the study were sometimes obscured by seemingly unrelated experiments, frequent mentions of what was not the aim of the study, grammatical errors, an awkward language.

Therefore, I recommend that minor revisions are implemented prior to publication.

Please see detailed comments and suggestions below.

### Major Comments

1. The authors should provide an explanation, either on Page 5 or in the Conclusion as to why they investigated this particular AAR from *Ca. A. phosphatis* rather than further characterizing one of the two NADH-preferring AARs previously published (de Las Heras

et al. 2016, Ling et al. 2018), both of which have enabled PHB production at high yield.

We modified the manuscript to illustrate with more clarity why we chose the AAR from *Candidatus Accumulibacter phosphatis* instead of the AAR from *Halomonas bluephagenesis* or *Allochromatium vinosum*. Citing:

“Looking for an NADH-preferring acetoacetyl-CoA reductase engaged in PHB accumulation, we decided to study the enzyme from the bacterium *Candidatus Accumulibacter phosphatis* (AAR<sup>CAp</sup>). The choice of this organism was based on the following observations. First, this organism is able to anaerobically convert acetate and glucose equivalents into PHB with full electron conservation (Figure 1C). Therefore, it naturally does what Carlson and co-workers found as the ideal scenario for anaerobic PHB accumulation. Second, genomic and transcriptomic data indicate that this organism lacks the enzymes catalyzing the reactions of the oxidative branch of pentose-phosphate pathway (11), a common source of NADPH. Furthermore, no gene encoding for an NADP<sup>+</sup>-depending non-phosphorylating glyceraldehyde-3-phosphate dehydrogenase was found in this bacterium. Therefore, oxidation of glucose equivalents should yield NADH. Third, if AAR<sup>CAp</sup> is an NADPH-preferring enzyme, electrons derived from glucose equivalents oxidation (carried as NADH) must be transferred to NADPH by some transhydrogenase mechanism. Given the redox potential of NAD(H) and NADP(H) pools, transfer of reducing equivalents from the former to the latter pool requires energy (12,13). A more parsimonious and energetically cheaper solution is to have an NADH-preferring acetoacetyl-CoA reductase.”

Different to the works of de Las Heras and co-workers (<https://doi.org/10.1186/s12934-016-0598-0>) and Ling and co-workers (<https://doi.org/10.1016/j.ymben.2018.09.007>), our focus was to confirm we have an AAR clearly preferring NADH over NADPH under physiologically relevant conditions. Indeed, our long-term objective is to increase the PHB yields under anaerobic/hipoxic conditions, where the cellular NADH/NAD ratio is higher than in the aerobic conditions. However, a key piece to generate PHB as a fermentation product, and to achieve this long-term objective, is to have a NADH-specific AAR.

Since the immediate objective is to find a *bona fide* NADH-preferring AAR capable to be engaged in PHB accumulation, there are at least three reasons to endorse the study of the AAR from *Ca. A. phosphatis* instead of using the AARs from *A. vinosum* or *H. bluephagenesis*.

First, although the AAR from *Halomonas bluephagenesis* or *Allochromatium vinosum* were claimed to be NADH-preferring, these claims were based on the comparison between initial

rates ( $v^{\text{NADH}}/v^{\text{NADPH}}$ ) obtained at a single concentration of acetoacetyl-CoA and NAD(P)H. Without available data of the  $K_M$  for acetoacetyl-CoA, NADH and NADPH; and without providing data of the activities at other substrate and cofactor concentrations, NADH preference of these enzymes should be considered an assumption rather than an actual observation.

Second, even if we assumed that  $v^{\text{NADH}}/v^{\text{NADPH}}$  is a suitable indicator of the *in vivo* cofactor usage by the AARs, the  $v^{\text{NADH}}/v^{\text{NADPH}} = 720/11 \approx 65$  observed in the cell-free extract from *Ca. A. phosphatis* is a value higher than the  $56/5 \approx 24$  observed in the cell-free extract from *H. bluephagenesis* or the  $185/39 \approx 5$  observed in the cell-free extract from the yeasts expressing the AAR from *A. vinosum*.

Third, according to several observations, *Ca. A. phosphatis* accumulates PHB in anaerobic conditions coupled to glycogen mobilization and acetate uptake. Different to *A. vinosum* or *H. bluephagenesis*, *Ca. A. phosphatis* does not have an NADPH-producing oxidative branch of the pentose-phosphate pathway. This way, the oxidation of glucose or glucose equivalents yields electrons carried only by NADH. Because PHB has a higher e-/C ratio than glucose, polymer accumulation could operate as a mechanism to re-oxidize NADH in such conditions. One way to enable this re-oxidation is having an NADH-preferring acetoacetyl-CoA reductase. Therefore, the ecological and biochemical conditions present during the PHB accumulation in *Ca. A. phosphatis* suggest the presence of an NADH-preferring AAR.

2. Figures 1B and 1C are unclear. First, the electrons marked in the figure do not match the description in the legend. The legend indicates that the formation of one monomer of HB requires only two electrons per every two acetyl groups, and that six electrons per glucose have to flow to another electron sink. Why then, do Figures 1B and 1C indicate 18 electrons per monomer under HB. Please explain this in the figure legend. Also, is the black line representative of the membrane? Is the white circle representative of the membrane bound transhydrogenase? These features should either be labeled in the figure or described in the legend. Making the line in Figure 1C from 6 Ac to 8 AcCoA dashed may help demonstrate that this involves transport of external acetate.

Both content and legend of Figure 1 were modified to fix the problems mentioned by the reviewer. See below:

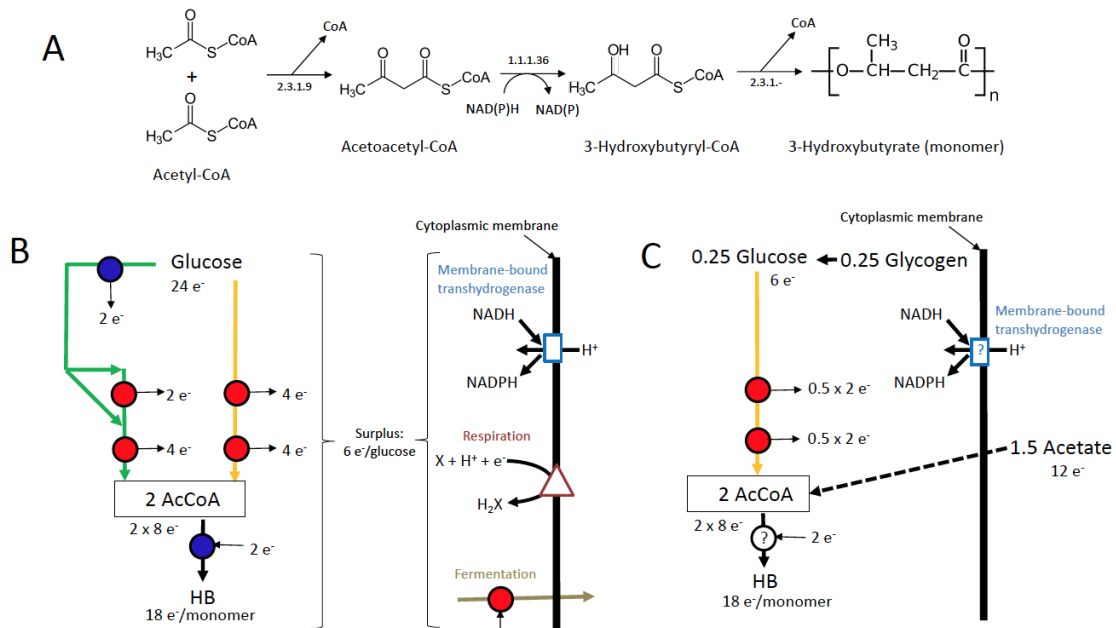


Figure 1: Electron transfer from carbon source(s) to PHB. NAD(H)-driven processes are represented by red circles and NADP(H)-driven processes by blue circles. **A:** PHB formation pathway. The enzymes catalyzing the steps involved in this conversion are identified using their Enzyme Commission (E.C.) codes. **B:** In the most studied cases—such as recombinant *E. coli* expressing *phaCAB* genes from *C. necator*—glucose is catabolized by Embden–Meyerhof (in orange) or Entner–Doudoroff pathway (in green), yielding two acetyl-CoA (AcCoA) per glucose and eight electrons carried by NADP<sup>+</sup> and/or NAD<sup>+</sup>. One monomer of hydroxybutyrate (HB) contains 18 electrons, and could be form from two acetyl-CoA (16 electrons) and two electrons carried by NADPH. Therefore, there is a surplus of six electrons per glucose that must flow to other electron acceptors (an external acceptor in the case of Respiration, an internally generated acceptor in the case of Fermentation). If glucose oxidation happens only through Embden–Meyerhof pathway, then participation of an energy-dissipating membrane-bound transhydrogenase is also required to transfer electrons from NADH to NADPH. **C:** In the case of *Ca. Accumulibacter phosphatis*, PHB formation takes place under anaerobic conditions. Acetyl-CoA is coming from an internal glycogen reserve and from external acetate, with full electron conservation. Acetate must be taken up and activated to become acetyl-CoA (several steps, represented with a dashed line). The genes encoding for the enzymes catalyzing the reactions of the oxidative branch of pentoses-phosphate pathway or Entner-Doudoroff pathway have not been found in this organism. If PHB accumulation is driven by NADPH, some transhydrogenase mechanism would be required. However, transhydrogenase activity has not been definitively confirmed. If PHB accumulation is driven by NADH, then NADH generated in the lower Embden–Meyerhof pathway could be used to drive PHB formation.

3. How confident are the authors that the AAR amplified from the enriched mixed culture is from *Ca. A. phosphatis* and not from another organism? Is it possible to isolate a pure culture of this organism? If not, the gene could be synthesized from the reference sequence CAP2UW1\_3919. At the least, the possibility that the AAR could also be from another unknown organism should be mentioned on Page 13

In the revised version, we discussed this issue based on the point raised by the reviewer. Citing:

“It had been impossible to isolate colonies of *Ca. A. phosphatis* so far, and it is likely that different closely related species are grouped under this taxonomic name. However, amino acid identity was over 93 % in all the sequenced clones. Moreover, the residues D94, K99, Y185, Q147 and Q150, identified as key residues for the enzymatic activity in AAR<sup>Cn</sup> (30), were conserved in the cloned sequences. Therefore, we considered those cloned genes as *phaB* homologues. Because the biological meaning of the observed DNA and protein polymorphism is not clear, for further characterization we chose the clone with the highest identity respect to the reference sequence: *phaB*<sup>CAp6</sup> (89 % DNA identity, 95 % amino acid identity). A group of amino acids relevant for cofactor specificity (see Section 3.3) in *phaB*<sup>CAp6</sup> was identical to the reference protein sequence.”

Because no pure cultures have been obtained, it could indeed happen that the characterized enzyme did not belong to *Ca. A. phosphatis*. It would have been possible to synthesize a gene identical to the reference sequence CAP2UW1\_3919. However, we considered the isolation of a homologue of CAP2UW1\_3919 directly from an actively PHB accumulating *Ca. A. phosphatis*-enriched culture as a more reliable option. The observed polymorphism (3 different sequences in 4 cloned genes) could be an interesting clue to follow-up in future studies.

4. The results from Table 2 need to be presented in the text. The only results mentioned are those for the competitive inhibition constant.

In the revised version of the manuscript, we included a more detailed discussion around the kinetic parameters. Citing:

“A compilation of the obtained kinetic parameters is presented in Table 2. The physical meaning of  $K_M$  parameters depends on the model employed to fit the related experimental data. The estimates of  $K_M^{\text{AcAcCoA}}$  and  $k_{cat}^{\text{AcAcCoA}}$  using NADH were obtained using the rapid-equilibrium model. The other kinetic parameters were obtained using the steady-state (Briggs-

Haldane) approach. As expected, the turnover constants ( $k_{cat}$ ) for each cofactor were very similar, either when obtained varying the concentrations of substrate or cofactor (Table 2). The individual analysis of the kinetic parameters enabled a first-sight comparison of the performances of AAR<sup>CAP</sup> using NADH or NADPH. Using NADH,  $K_M$  of both substrate and cofactor were lower,  $k_{cat}$  was higher, and NAD<sup>+</sup> inhibited the rates less than NADP<sup>+</sup>. Cofactor preference is often expressed as the ratio between the catalytic efficiencies ( $k_{cat}/K_M$ ) estimated for each cofactor. A comparison between the acetoacetyl-CoA reductases that had been kinetically characterized showed that AAR<sup>CAP</sup> has the lowest  $k_{cat}/K_M$  for NADPH and the second highest  $k_{cat}/K_M$  for NADH, only after the homologue from *Halomonas boliviensis* (see Supplementary Table 4). However, the  $k_{cat}/K_M$  for NADPH of the acetoacetyl-CoA reductase from *H. boliviensis* is almost three times higher than its  $k_{cat}/K_M$  for NADH. Therefore, according to such criterion, the acetoacetyl-CoA reductase from *H. boliviensis* is not a NADH-preferring enzyme.

Anyways, it is important to highlight that, for multi-substrates reactions, the comparison between the  $k_{cat}/K_M$  obtained with different substrates or cofactors reflects better the preference when the concentration of the co-substrate is saturating, a situation not necessarily occurring under physiological conditions. In our specific case, the low  $K_{ic}^{NAD(P)}$  values indicate that *in vivo* AAR<sup>CAP</sup> activity should be highly dependent on NAD(P) concentration and, therefore, on NAD(P)H/NAD(P) ratios. Because these ratios depend on the physiological conditions, cofactor preference is a dynamic property rather than a static number. For the calculation of this dynamic preference, we implemented a quantitative approach considering the variation of NAD<sup>+</sup>, NADP<sup>+</sup>, NADH, and NADPH concentrations inside physiologically feasible ranges.”

Moreover, we used those kinetic parameters to quantify the relative use of NADH and NADPH under the dynamic physiological conditions. We calculated the use of NADH over NADPH both through the conventional comparison between the specificity constants ( $k_{cat}/K_M$ ) and through a more detailed equation including the competition between the alternative substrates NADH and NADPH, and the competition of the products NAD and NADP. The result of this quantitative approach is shown in the Figure 2 of the revised manuscript. The most relevant conclusion is that the studied enzyme will largely prefer NADH at physiological conditions.

5. I am not confident about the conclusions the authors draw from the results in Table 3. First, the kinetic parameters from the two sources provided are extremely different in magnitude. Also, these cannot be compared directly to the measurements conducted in this study for the AAR chimera because the experimental conditions are different. For this comparison



to be done properly, the kinetic parameters for the native AAR from *C. necator* should be measured under the same experimental conditions as for the chimera.

In the reviewed version of the manuscript we are including additional data: NADH- and NADPH-linked specific acetoacetyl-CoA reductase activities from cells over-expressing the acetoacetyl-CoA reductases from *C. necator*, *Ca. A. phosphatis* and Chimera, obtained under the same experimental conditions (see Table 3 of the revised manuscript).

Regarding the differences between the kinetic parameters of AAR<sup>Cn</sup> reported in the two cited sources, we added:

“In the case of AAR<sup>Cn</sup>, kinetic parameters obtained with purified enzyme were found in the reports of Haywood and co-workers (29) and Matsumoto and co-workers (45). While Matsumoto and co-workers characterized the enzyme activity using only NADPH, Haywood and co-workers studied the activities with NADH and NADPH. Then, we chose the data reported by the latter to compare the cofactor preferences among AAR<sup>Cn</sup>, AAR<sup>Chimera</sup> and AAR<sup>CAp</sup> using the parameter  $(k_{cat}/K_M^{NADH}) / (k_{cat}/K_M^{NADPH})$  (Table 3). Despite the differences between the kinetic parameters reported by Haywood and co-workers and Matsumoto and co-workers, their estimates of  $(k_{cat}/K_M^{NADPH})$  are similar ( $2.62 \times 10^5 \text{ M}^{-1}\text{s}^{-1}$  and  $6.85 \times 10^5 \text{ M}^{-1}\text{s}^{-1}$ , respectively). Therefore, either comparing the observations from Haywood and co-workers or Matsumoto and co-workers, our conclusion about the shift in cofactor specificity in AAR<sup>Chimera</sup> respect to the parental AAR<sup>Cn</sup> would be qualitatively similar.”

6. The modeling experiments to identify potential bottlenecks were distracting from the main purpose of the paper. The authors write several times that the point of the paper was not to achieve high PHB titers; however, the modeling experiments seem like an attempt to do just that. I think the paper would be more cohesive if it focused on the new AAR enzyme, its characterization, and proof of its in vivo activity, rather than trying to identify bottlenecks (which, is typically a strategy to achieve high titers). I would suggest writing a separate paper about the modeling component, which will also give the authors the necessary space to adequately describe the model and all of the information that it provided.

We followed the advice of the reviewer and excluded the modeling approaches here. We are co-submitting a Data in Brief article where the modeling aspects are shown with more details. We removed the analysis of putative bottlenecks derived from the comparison between model and experimental results. In consequence, a more compact Conclusion section is presented in the revised version.

7. I recommend removing all instances where the authors explain what the aim of the study is not, and instead focus on what the aim of the study is.

We agree. We think the importance and novelty of our analyses and results are more clear in the revised version.

#### Minor Comments

1. Lack of clarity and/or progression of the text:

- The progression of the text at the top of Page 5 is confusing. I recommend removing the sentence “However, another problem arise when considering the best studied PHB pathway,” and modifying the next sentence to read “While genes encoding for the enzymes required for the conversion of acetyl-CoA to PHB have been identified in many organisms, it was not until the successful expression of the operon *phaCAB* from *Cupriavidus necator* in *E. coli* that there was significant interest in metabolic engineering for PHB accumulation.”

The section Introduction was modified. We think the progression of the text and motivation are more clear now.

In the Introduction:

“The direct use of NADH to drive the reduction of acetoacetyl-CoA to R-3-hydroxybutyryl-CoA has basic and applied implications. From the basic science perspective, it would mean that *Ca. A. phosphatis* developed a mechanism to transfer electrons from glycolysis to PHB accumulation without involving an energy-consuming transhydrogenase. From the applied science perspective, it would mean that PHB can be produced as a fermentation product, avoiding competition for NADPH between biomass and PHB accumulation.

Aiming to find a bona fide NADH-preferring acetoacetyl-CoA reductase suitable for PHB accumulation, we characterized here the cofactor preference of an acetoacetyl-CoA reductase obtained from a *Ca. A. phosphatis*-enriched mixed culture. Moreover, we investigated the role of some key residues in the cofactor discrimination and we observed engagement of this enzyme in PHB accumulation.”

In the Conclusion:

“In this research, we identified and characterized an acetoacetyl-CoA reductase that prefers NADH over NADPH in a wide range of physiologically feasible NAD(P)(H) concentrations. Moreover, a structural analysis and further kinetic characterization of a mutant enzyme indicated a group of key amino acids with a relevant role in the observed cofactor specificity, opening the way to further protein engineering approaches and to the quest for other NADH-specific acetoacetyl-CoA reductases in other (meta)genomes. Finally, evidence of engagement of this NADH-preferring acetoacetyl-CoA reductase in PHB accumulation was shown.”

- The last sentence on Page 13 in Section 3.1 does not fit with that paragraph, and seems unnecessary.

Fixed

- A topic sentence is needed to start Section 3.2 that tells the reader from where the DNA is being amplifying. I assumed this was from the enriched-mixed culture, but it was not obvious.

Fixed

- On Page 15, it makes more sense to compare the kinetic parameters found in Table 2 to those of other homologs (Supplementary Table 7) before discussing the impact of different NAD(P)H/NAD(P)<sup>+</sup> ratios on cofactor preference.

Fixed.

- The last sentence of the first paragraph on Page 18 is misleading. It makes it seem like the authors have already presented results detailing PHB accumulation. It might be helpful to write something like “We next sought to link the accumulation of PHB to the presence of the operon [...] in order to provide evidence of (1) the ability [...] and (2) the functionality of the artificial operon in vivo.”

Fixed

- Based on the legend for Supplementary Figure 6, the first sentence of the last paragraph on Page 18 should indicate that low activity was “observed in E. coli cell extracts” rather than “cells.”

Fixed

- On Page 19, it would be clearer to write “Given the inability of wild-type E. coli to produce PHB, the observed accumulation of PHB confirmed the ability of the AARCAp to be engaged in PHB accumulation [...].”

Fixed

2. In Supplementary Table 7, units must be provided for kcat/KM. KM is given in units of mM but the kcat/KM is calculated using KM values in μM.

Fixed

3. Throughout the manuscript, NAD<sup>+</sup> and NADP<sup>+</sup> are consistently denoted without the + charge. This + should be added in the text and figures for accuracy.

Fixed, including Supplementary material.

4. The use “experimental model” is misleading, as this seems to imply a computational model, rather than an engineered organism.

Fixed

5. Awkward wording throughout the manuscript. For example:

- Page 4: Oxygen is described as a major “sink of the electrons.” Oxygen can more clearly be described as an “electron sink.”
- Page 4: “Carlson and co-workers made a study of” should read “Carlson and coworkers studied.”

Fixed

6. There were several grammatical errors throughout the manuscript that should be corrected before publication. For example:

- Page 4: The last line of the first paragraph of the Introduction should read “Given all of these disadvantages, why is oxygen so commonly used in PHB production processes?” There were previously several errors in this sentence.
- Page 18: “However, the observed NADH-linked AAR activity (Supplementary Figure 6) not necessarily guaranteed [...]” is not grammatically correct. It should read “However, the observed NADH-linked AAR activity (Supplementary Figure

6) does not necessarily guarantee [...].”

Fixed

7. Several times throughout the manuscript the word “the” is used in excess. These should be removed. For example:

- Page 6: “transfer electrons from the glycolysis to the PHB accumulation” should instead read “transfer electrons from glycolysis to PHB accumulation.”
- Page 7: “avoiding the competition for NADPH between the biomass and the PHB accumulation” should instead read “avoiding competition for NADPH between biomass and PHB accumulation.”

Fixed

#### Reviewer #2:

In this manuscript authors tried to develop NADH preferring Acetoacetyl CoA reductase (AAR). They characterized *Ca. A. phosphatis* AAR and found the AAR in this organism is type of NADH preferring enzyme. From the 3D structure analysis of the enzyme and comparison of the enzyme with NADPH preferring AAR, they tried to find some key residues. The AAR\_Chimera was constructed, following their hypothesis and NADH preferring characteristics was observed. The AAR\_Chimera was used for production of PHB in *E. coli*. Co-factor preference of NADH and NADPH is a important problem to produced reducing power required compounds, I agree with importance of the subject in the study. As authors recognized well the idea of PHB production by NADH preferring AAR is not new (Chen 2018), novelty of the study should be clarified.

AAR<sup>Chimera</sup> was not used to test the NADH-driven PHB accumulation, the wild type AAR<sup>CAp</sup> was used for that purpose.

In the revised version of the manuscript we explained why the information available in the reports from De las Heras and co-workers and Ling and co-workers is not enough to claim that the acetoacetyl-CoA reductases from *Allochromatium vinosum* and *Halomonas bluephagenesis* are NADH specific. Citing:

“Previous publications reported the use of NADH-preferring acetoacetyl-CoA reductases from *Allochromatium vinosum* and *Halomonas bluephagenesis* for PHB accumulation (6,7). However, in those studies the cofactor preference was evaluated through a comparison between activities obtained at a single substrate and a single cofactor concentration. Moreover, product inhibition by NAD<sup>+</sup> and NADP<sup>+</sup> were not evaluated, and saturation constants were not reported. Considering that, *in vivo*, NADPH/NADP<sup>+</sup> and NADH/NAD<sup>+</sup> ratios are different (8) and that these ratios change depending on physiological conditions (9,10), the assessment of the cofactor preference of any acetoacetyl-CoA reductase should be evaluated at physiologically meaningful NADPH/NADP<sup>+</sup> and NADH/NAD<sup>+</sup> ratios. Therefore, the information provided in those previous reports is not enough to ensure the use of NADH over NADPH under physiological conditions.”

The key novel results of our work are:

- First kinetic characterization of a true NADH-preferring AAR, including estimations of  $k_{cat}$ ,  $K_M$  (for acetoacetyl-CoA, NADH and NADPH) and  $\text{NAD(P)}^+$  inhibition constants.
- The role of key amino acids in the cofactor discrimination was experimentally tested.

1. By three-D structure analysis based on homology modeling, they hypothesized some important residues. Consideration about steric hindrance of NADPH into the pocket of AAR, not only N37 and R41 but also K40, F38 were significant for preference of NADH in their discussion. However, they chose only these two residues. Why authors showed the experimental results of E37 and P41 chimera AAR. They should investigate effect of replacement of K40 and F38. Especially F38 replacement should be done. Additionally why (N37 and R41)->(E37 and P41) is only tried? Other residues candidates are not chosen? Systematic analysis based on the simulation and experiments should be done for possible or all candidates of residues replacement. Otherwise I think it is difficult to claim the novelty of the manuscript.

Although previous reports pointed to the presence of the E37 residue as a key structural determinant for the use of NADH by the acetoacetyl-CoA reductases, these hypotheses were not experimentally tested. We designed and studied the artificial enzyme Chimera to experimentally verify the role of the residues present in the loop connecting the secondary structures  $\alpha_2$  and  $\beta_2$  in the acetoacetyl-CoA reductases. Our strategy was to substitute a fragment embracing five residues instead of studying the results of single residue mutations.

Certainly, a deeper comprehension of the structural determinants of the cofactor specificity of the acetoacetyl-CoA reductases will require a systematic study by site-directed mutagenesis of different individual positions and probably changing more than one residue. With the present work we only wanted to advance one step more in the direction of the identification of the key residues determining the cofactor specificity in this family. Chimera showed a  $(k_{cat}/K_M^{\text{NADH}}) / (k_{cat}/K_M^{\text{NADPH}})$  475 times higher than the parental acetoacetyl-CoA reductase from *C. necator*. Then, we think we identified something relevant for the determination of cofactor preference. Given that our main objective was not to revert the cofactor specificity of the acetoacetyl-CoA reductase from *C. necator* but to find a NADH-preferring acetoacetyl-CoA reductase engaged in PHB accumulation, we think we succeeded in that objective.

On the other hand, compared to previous work, our phylogenetic analysis includes a more detailed observation of the sequence motifs in the cofactor binding site of the acetoacetyl-CoA reductase. Also, our conclusions about the structural determinants influencing the cofactor

preference are different to the conclusions of De las Heras and co-workers (2016) and Chen and co-workers (2018).

2. Authors showed the effectiveness of chimera protein for production of PHB. Authors should show the PHB production by *E. coli* with AAR gene of *C. necator*. This enzyme is NADH preferring AAR. I think this result should be essential.

The specific purpose of Chimera was to study the role of the residues present in the loop connecting the secondary structures  $\alpha_2$  and  $\beta_2$ . However, our main objective was to find a NADH-preferring acetoacetyl-CoA reductase engaged in PHB accumulation. The expression of the acetoacetyl-CoA reductase from *C. necator* would not be useful for that main objective because it is not an NADH preferring AAR (see Table 3 of the revised version). Moreover, PHB accumulation in *E. coli* cells expressing the acetoacetyl-CoA reductase from *C. necator* has been tested elsewhere, including the observation of the effects of reducing oxygen supply and deletion of competing by-products (for example: <https://doi.org/10.1007/s00253-008-1816-4> ; <https://doi.org/10.1155/2015/789315>).

Anyways, we do have unpublished data of recombinant *E. coli* cells expressing the *phaCAB* genes from *C. necator*, growing in a continuous culture (dilution rates near  $0.1 \text{ h}^{-1}$ ), at different levels of oxygen limitation (see Table below with the specific consumption/production rates). These are the same conditions employed in the continuous culture reported in the manuscript under revision. It is possible to observe that, contrary to the case where PHB formation is driven by NADH, PHB accumulation decreased with the reduction in the oxygen supply.

Dilution rate ( $\text{h}^{-1}$ )	$0.092 \pm 0.003$	$0.096 \pm 0.006$	$0.091 \pm 0.005$	$0.090 \pm 0.003$
Glucose consumption rate (mmol/gCDW/h)	$3.034 \pm 0.071$	$2.882 \pm 0.067$	$2.567 \pm 0.060$	$2.506 \pm 0.039$
<b>Oxygen consumption rate (mmol/gCDW/h)</b>	<b><math>4.681 \pm 0.097</math></b>	<b><math>4.431 \pm 0.208</math></b>	<b><math>3.536 \pm 0.107</math></b>	<b><math>2.638 \pm 0.113</math></b>
CO <sub>2</sub> production rate (mmol/gCDW/h)	$6.247 \pm 0.128$	$4.695 \pm 0.223$	$4.265 \pm 0.125$	$2.910 \pm 0.122$
Acetate production rate (mmol/gCDW/h)	$1.253 \pm 0.137$	$1.281 \pm 0.072$	$1.416 \pm 0.116$	$1.726 \pm 0.072$
Ethanol production rate (mmol/gCDW/h)	$1.499 \pm 0.103$	$0.795 \pm 0.051$	$0.879 \pm 0.067$	$0.685 \pm 0.026$
Glycerol production rate (mmol/gCDW/h)	$0.428 \pm 0.038$	$0.610 \pm 0.034$	$0.394 \pm 0.031$	$0.458 \pm 0.020$
Formate production rate (mmol/gCDW/h)	$1.071 \pm 0.160$	$2.452 \pm 0.147$	$1.437 \pm 0.127$	$1.989 \pm 0.096$
Succinate production rate (mmol/gCDW/h)	$0.012 \pm 0.003$	$0.013 \pm 0.001$	$0.0087 \pm 0.0004$	$0.030 \pm 0.007$
<b>PHB production rate (mmol/gCDW/h)</b>	<b><math>0.077 \pm 0.002</math></b>	<b><math>0.055 \pm 0.003</math></b>	<b><math>0.048 \pm 0.002</math></b>	<b><math>0.039 \pm 0.001</math></b>
qO <sub>2</sub> /qS	$1.543 \pm 0.048$	$1.537 \pm 0.081$	$1.377 \pm 0.053$	$1.053 \pm 0.048$

These results were not included in this manuscript because they belong to another ongoing research project and because they will take the focus out of what is important in this

manuscript: to show that we found a bona fide NADH-preferring acetoacetyl-CoA reductase and to show that this enzyme can participate in PHB accumulation.

3. Authors showed kinetic parameters of NADPH-preferring AAR and AAR\_Chimera. However, they did not show the NADH and NADPH concentrations in the cell of *E. coli*. They should discuss AAR\_Chimera is effectively working in the cell or not from the view point of KM and NADH concentration. I think function of AAR in vivo should be discussed carefully. FBA and FVA cannot discuss kinetic behavior of AAR\_Chimera. I am not sure whether KM value of AAR\_Chimera is small enough for functioning this enzyme in vivo.

In the revised version, we explicitly quantified the influence of NAD<sup>+</sup>, NADH, NADP<sup>+</sup> and NADPH concentrations on the relative use of NADH and NADPH (cofactor specificity) and on the metabolic flux that the reaction catalyzed by AAR<sup>Cap</sup> can sustain (flux capacity). Citing:

“For our quantitative approach, we applied the generic BiBi rate equation proposed by Rohwer and co-workers (34). Using this generic equation, the rate of NADH consumption in the reaction catalyzed by AAR<sup>Cap</sup> can be written as:

$$v_{NADH} = \frac{k_{cat}^{NADH} * E * \frac{NADH * AcAcCoA}{K^{NADH} * K^{AcAcCoA}} * \left(1 - \frac{NAD * 3HBCoA}{NADH * AcAcCoA * K_{eq}}\right)}{\left(1 + \frac{NADH}{K^{NADH}} + \frac{3HBCoA}{K^{3HBCoA}}\right) * \left(1 + \frac{AcAcCoA}{K^{AcAcCoA}} + \frac{NAD}{K^{NAD}}\right)}$$

where  $K^{NADH}$ ,  $K^{AcAcCoA}$ ,  $K^{3HBCoA}$  and  $K^{NAD}$  are dissociation constants associated to the interactions between the corresponding ligands and different forms of the enzyme. However, *in vivo*, NAD<sup>+</sup> and NADH binding will be affected by NADP<sup>+</sup> and NADPH concentrations because they can also bind to the enzyme. Considering NADPH and NADP<sup>+</sup> as competitive inhibitors of NADH and NAD<sup>+</sup> binding, the terms  $K^{NADH}$  and  $K^{NAD}$  were multiplied by the factor

$\left(1 + \frac{NADPH}{K^{NADPH}} + \frac{NADP}{K^{NADP}}\right)$ . After introducing such modifications, the equation was written as:

$$v_{NADH} = \frac{k_{cat}^{NADH} * E * \frac{NADH * AcAcCoA}{K^{NADH} * \left(1 + \frac{NADPH}{K^{NADPH}} + \frac{NADP}{K^{NADP}}\right) * K^{AcAcCoA}} * \left(1 - \frac{NAD * 3HBCoA}{NADH * AcAcCoA * K_{eq}}\right)}{\left(1 + \frac{NADH}{K^{NADH} * \left(1 + \frac{NADPH}{K^{NADPH}} + \frac{NADP}{K^{NADP}}\right)} + \frac{3HBCoA}{K^{3HBCoA}}\right) * \left(1 + \frac{AcAcCoA}{K^{AcAcCoA}} + \frac{NAD}{K^{NAD} * \left(1 + \frac{NADPH}{K^{NADPH}} + \frac{NADP}{K^{NADP}}\right)}\right)}$$

It is important to notice that we explored the effects of free concentrations of NAD<sup>+</sup>, NADH, NADP<sup>+</sup> and NADPH keeping in mind two important rules: (i) cofactor concentrations have to fulfill thermodynamic constraints and (ii) the sum of concentrations (NAD<sup>+</sup> + NADH) and (NADP<sup>+</sup> + NADPH) were considered as conserved moieties. Citing:

“However, beyond the availability of the required kinetic parameters, to obtain a physiologically meaningful result, it is important to evaluate the rate expressions with physiologically feasible substrate, product and cofactors concentrations. Because their ability of binding to other bio-molecules, free NAD(P)(H) concentrations are difficult to measure, and many experimentally reported values represent thermodynamically unfeasible states, as demonstrated by Canelas and co-workers (37). To overcome these problems, we calculated cofactor concentration ranges consistent with the thermodynamic constraints enabling the operation of glycolysis (38,39). In the case of NADH / NAD<sup>+</sup> ratios, it is known that these values depend on the redox potential of the available electron acceptor (9). This way, we explored NADH / NAD<sup>+</sup> ratios in the range between 0.03 (fully aerobic) and 0.71 (no external electron acceptor), according to experimentally determined values (9). Regarding the NADPH / NADP<sup>+</sup> ratios, there is a wide range of reported values in literature, from 0.32 (40) to 60 (41). Total moieties sizes of (NAD<sup>+</sup> + NADH) = 1470 + 100 = 1570 μM and (NADP<sup>+</sup> + NADPH) = 195 + 62 = 257 μM were considered, according to the data from Chassagnole and co-workers (40). Therefore, to calculate the ranges of individual cofactors concentrations, the following systems of simple algebraic equations were solved:

	NAD(H)	NADP(H)
More oxidized moiety	$\frac{\text{NADH}}{\text{NAD}} = 0.03$ (I) $\text{NAD} + \text{NADH} = 1570$ (II) Solutions: NAD = 1524 μM; NADH = 46 μM	$\frac{\text{NADPH}}{\text{NADP}} = 0.32$ (I) $\text{NADP} + \text{NADPH} = 257$ (II) Solutions: NADP = 195 μM; NADPH = 62 μM
More reduced moiety	$\frac{\text{NADH}}{\text{NAD}} = 0.71$ (I) $\text{NAD} + \text{NADH} = 1570$ (II) Solutions: NAD = 918 μM; NADH = 652 μM	$\frac{\text{NADPH}}{\text{NADP}} = 60$ (I) $\text{NADP} + \text{NADPH} = 257$ (II) Solutions: NADP = 4 μM; NADPH = 253 μM

Anyways, the most important evidence of *in vivo* functionality of the enzyme AAR<sup>Cap</sup> is the observed accumulation of PHB.

Remarkably, the estimated maximum flux that AAR<sup>Cap</sup> activity can sustain calculated using the kinetic parameters and the measured specific activity (0.08 mmol/gCDW/h, see Supplementary Figure 5) is very similar to the observed maximum PHB accumulation flux (0.0676 mmol/gCDW/h, see Table 4).



Reviewer #3:

General comments:

Manuscript presents characterization of NADH-preferring acetoacetyl-CoA reductase and the artificial operon expression in *Escherichia coli* showed continuous poly(3-hydroxybutyrate) accumulation under oxygen limiting condition fermentation. The authors conducted enzyme activity and kinetic parameters evaluation, poly(3-hydroxybutyrate) production with engineered *E. coli* continuous fermentation and metabolic flux balance analysis. This study seemed interesting, however, there are several issues to be answered.

1. There are too much information and explanation at supplementary materials and annex to get clear data. I suggest that you should simplify information at supplementary materials and separate supplementary figures from materials explanation.

The number of Supplementary Materials was reduced from nine to four. Moreover, all the annexes were suppressed. Plasmids sequence maps were deposited in an online available database ("NADH-driven polyhydroxybutyrate accumulation in *E. coli* dataset 2" at Mendeley Data). Other former supplementary materials are co-submitted as a Data in Brief article, an option available in this journal.

2. In manuscript, there are many comments "artificial operon" which we do not use them for genetic engineering and it should be changed. We do not use the term artificial operon because genetic engineering used the genes from difference sources.

We eliminated the adjective "artificial" when mentioning the operon resulting from the non-natural assembly of *phaCA* genes from *C. necator* and the *phaB* gene from *Ca. A. phosphatis* under the control of the T7 promoter.

3. The title gave wrong information. Is only NADH-preferring acetoacetyl-coA reductase enables the generation of PHB? It should be careful to emphasize.

New title: An NADH preferring acetoacetyl-CoA reductase is engaged in poly-3-hydroxybutyrate accumulation in *Escherichia coli*

4. Although authors supplied a lot of data, it showed very simple story line without concrete conclusion and results. They simply found new strain and found out which amino acid is

important. Then, they produce very small amount of PHB. Overall contents should be shortened and well organized.

In the revised version, we show more clearly our objective. Citing: "Aiming to find a *bona fide* NADH-preferring acetoacetyl-CoA reductase suitable for PHB accumulation, we characterized here the cofactor preference of an acetoacetyl-CoA reductase obtained from a *Ca. A. phosphatis*-enriched mixed culture. Moreover, we investigated the role of some key residues in the cofactor discrimination and we observed engagement of this enzyme in PHB accumulation".

Despite the apparent simplicity of this goal, previous reports claiming the use of NADH preferring acetoacetyl-CoA reductases for PHB accumulation failed to show the evidence required to endorse the claimed use of NADH under the physiological conditions, only showing specific activities at a single substrate and NAD(P)H concentration, and without exploring the effects of physiologically relevant products such as NAD<sup>+</sup> and NADP<sup>+</sup>.

We are providing kinetic parameters enabling a quantitative assessment of the relative use of NADH and NADPH in the dynamic cellular conditions. Different to previous studies claiming the use of NADH preferring acetoacetyl-CoA reductases, the identification of key residues determining the observed cofactor specificity was experimentally tested. Finally, our results not only provide a key piece for further metabolic engineering efforts, they also help to understand the physiological role of PHB accumulation in *Candidatus Accumulibacter phosphatis*, an important organism in wastewater treatment.

About the amount of PHB produced, see the answer to the point number 6, where the issue of PHB content is raised again.

5. Result part of 3.5 should be deleted because it did not give any informative data on experiments.

This section was deleted.

6. Although many approaches and explanation were performed, increased PHB accumulation with engineered *E. coli* showed very low content and titer of PHB. Is *phaB* important or bottleneck of PHB synthesis and is the change of NADH-preferring acetoacetyl-CoA reductase meaningful?

In the revised version, we included an analysis of the *in vivo* functionality of the acetoacetyl-CoA reductase, including a calculation of the flux that AAR<sup>CAP</sup> can sustain. This calculation was based on the *in vitro* measured acetoacetyl-CoA reductase activity and the kinetic properties of this enzyme. This kinetic analysis shows that the observed PHB production flux was very

close to the flow capacity of the reaction catalyzed by AAR<sup>CAp</sup>, showing the importance of a careful kinetic characterization and the use of continuous cultures to identify bottlenecks.

Regarding the meaning of using an NADH preferring instead of an NADPH preferring acetoacetyl-CoA reductase, and the low PHB titers obtained by us, it is important to highlight that:

- (i) To achieve PHB contents of 50% or more in *E. coli* does not represent a technological challenge anymore, as proven elsewhere by different groups. The trick is to overexpress the *phaCAB* genes from *C. necator* and growth the resulting recombinant *E. coli* in batch or feed-batch using a medium rich in glucose and poor in nitrogen source. This creates a situation of metabolic overflow and due to the lack of nitrogen to make amino acids and nucleotides, biosynthesis is halted and NADPH is available for the PHB formation pathway. However, using NADPH preferring acetoacetyl-CoA reductases means a competition between growth and product formation. Therefore, the best growers are the worst producers. This eventually lead to instability in the production yield.
- (ii) As stated both in the original and the revised version, the achievement of higher PHB titers and lower production cost, using either an NADH or an NADPH preferring acetoacetyl-CoA reductase, will require further metabolic engineering efforts to achieve the required match between the catabolic supply of acetyl-CoA and NAD(P)H and the demand of the PHB formation pathway. The acetyl-CoA and NAD(P)H yields of the Embden-Meyerhof pathway or the Entner-Doudoroff pathway are not in the stoichiometric proportion required to make PHB. This eventually lead to the use of oxygen as a required electron sink, the use of a second carbon source or the production of a second product next to the PHB. None of these alternatives is fully satisfactory from the industrial point of view. However, the required metabolic engineering efforts to fix this mismatch are beyond the scope of the presented work.

7. Comparison with NADH-preferring acetoacetyl-CoA reductase and NADPH-preferring acetoacetyl-CoA reductase will be very helpful to claim author's points.

Reviewer 2 (point 2) raised exactly the same issue. Please, see the answer given to him/her above.

8. In table 2, the data should be shown with scientific way, not [6.74...8.67]

Fixed. In the case of non-linear fitting, confidence intervals are not necessarily symmetric around the best fitted value. This is why we are not using here the notation mean  $\pm$  standard deviation.

9. In Figure legends, the word "panel" should be removed.

Fixed.

10. In Fig.1, B and C were not informative.

Figures 1B and 1C were modified upon request of Reviewer 1 (Point 2). The idea of these figures is to visualize the stoichiometric relationships between the glycolytic pathways and the PHB formation pathway, with focus in the reducing equivalents and acetyl-CoA. In the case of the metabolisms represented in Figure 1B, it becomes clear the mismatch leading to the use of oxygen and the generation of other products beyond PHB. In the case of Figure 1C, it shows the case of *Ca. A. phosphatis*. This peculiar microorganism has the capacity (as illustrated in Figure 1C) of conserving all the reducing equivalents released during the glycolysis as PHB. The NADH preference of its acetoacetyl-CoA reductase is consistent with this particular trait. Therefore, we think that Figure 1 is indeed very important for the message we want to transmit.

11. Fig 3 was hard to read and the main idea should be emphasized in Figure. Or, it should be removed with section 3.5.

The mentioned figure was removed.

## Highlights

- We studied an acetoacetyl-CoA reductase with the highest NADH-preference so far described.
- Residues between E37 and P41 are key for the NADH preference.
- The expression of this enzyme enabled production of PHB as a fermentation product in *Escherichia coli*.

**Title:** An NADH preferring acetoacetyl-CoA reductase is engaged in poly-3-hydroxybutyrate accumulation in *Escherichia coli*

Running title: NADH-driven PHB accumulation in *E. coli*

Authors: Karel Olavarria<sup>a</sup>, Alexandre Carnet<sup>a</sup>, Joachim van Ranselaar<sup>a</sup>, Caspar Quakkelaar<sup>a</sup>, Ricardo Cabrera<sup>b</sup>, Leonor Guedes da Silva<sup>a</sup>, Aron L. Smids<sup>a</sup>, Pablo Villalobos<sup>b</sup>, Mark C.M. van Loosdrecht<sup>a</sup>, and S. Aljoscha Wahl<sup>a</sup>

Affiliations:

<sup>a</sup>: Departement Biotechnologie, Faculteit Technische Natuurwetenschappen, Technische Universiteit Delft. Van der Maasweg 9, 2629 HZ, Nederlands. Telephone: +31-152783193

<sup>b</sup>: Departamento de Biología, Facultad de Ciencias, Universidad de Chile. Las Palmeras 3425, Ñuñoa, Región Metropolitana, Chile.

E-mail addresses:

Karel Olavarria: [k.olavarriagamez@tudelft.nl](mailto:k.olavarriagamez@tudelft.nl) (corresponding author)

Alexandre Carnet: [carnetalexandre@gmail.com](mailto:carnetalexandre@gmail.com)

Joachim van Ranselaar: [joachimvrens@gmail.com](mailto:joachimvrens@gmail.com)

Caspar Quakkelaar: [casparquakkelaar@hotmail.com](mailto:casparquakkelaar@hotmail.com)

Ricardo Cabrera: [ricabrer@uchile.cl](mailto:ricabrer@uchile.cl)

Leonor Guedes da Silva: [leonorsilva28@gmail.com](mailto:leonorsilva28@gmail.com)

Aron L. Smids: [aronragtag@msn.com](mailto:aronragtag@msn.com)

Pablo Villalobos: [pavillalobos@u.uchile.cl](mailto:pavillalobos@u.uchile.cl)

Mark C.M. van Loosdrecht: [M.C.M.vanLoosdrecht@tudelft.nl](mailto:M.C.M.vanLoosdrecht@tudelft.nl)

S. Aljoscha Wahl: [S.A.Wahl@tudelft.nl](mailto:S.A.Wahl@tudelft.nl)

## Abstract

Oxygen supply implies higher production cost and reduction of maximum theoretical yields. Thus, generation of fermentation products is more cost-effective. Aiming to find a key piece for the production of (poly)-3-hydroxybutyrate (PHB) as a fermentation product, here we characterize an acetoacetyl-CoA reductase, isolated from a *Candidatus Accumulibacter phosphatis*-enriched mixed culture, showing a  $(k_{\text{cat}}^{\text{NADH}}/K_{\text{M}}^{\text{NADH}})/(k_{\text{cat}}^{\text{NADPH}}/K_{\text{M}}^{\text{NADPH}}) > 500$ . Further kinetic analyses indicate that, at physiological concentrations, this enzyme clearly prefers NADH, presenting the strongest NADH preference so far observed among the acetoacetyl-CoA reductases. Structural and kinetic analyses indicate that residues between E37 and P41 have an important role for the observed NADH preference. Moreover, an operon was assembled combining the *phaCA* genes from *Cupriavidus necator* and the gene encoding for this NADH-preferring acetoacetyl-CoA reductase. *Escherichia coli* cells expressing that assembled operon showed continuous accumulation of PHB under oxygen limiting conditions and PHB titer increased when decreasing the specific oxygen consumption rate. Taken together, these results show that it is possible to generate PHB as a fermentation product in *E. coli*, opening opportunities for further protein/metabolic engineering strategies envisioning a more efficient anaerobic production of PHB.

**Keywords:** acetoacetyl-CoA reductase; NADH; NADPH; oxygen limitation; cofactor specificity; Polyhydroxybutyrate

## 1. Introduction

Although (poly)-3-hydroxybutyrate (PHB) was discovered almost 100 years ago (1), studies focused on this polymer have recently burgeoned in response to increasing interest in environment-friendly materials to replace non-biodegradable plastics. However, PHB production cost is still high if compared with fossil-fuel based plastics. One of the factors affecting PHB production cost is the required oxygen supply (Figure 1). Oxygen supply implies not only extra material and energy input: oxygen itself is also a major electron sink, reducing product yield (2).

Carlson and co-workers studied the maximum theoretical PHB yield under anaerobic conditions, given the glycolytic pathways available in *Escherichia coli* (3). They concluded that co-feeding glucose and acetate with a 2:1 ratio, it is possible to co-generate two 3-hydroxybutyryl monomers and two formate, approaching a carbon yield of 0.8. Remarkably, for their theoretical analysis, Carlson and co-workers assumed an NADH-consuming PHB production pathway. Acknowledging that best studied PHB synthesis pathways include an NADPH-preferring instead of an NADH-preferring acetoacetyl-CoA reductase, they included in their theoretical network a transhydrogenase catalyzing the transference of electrons from NAD(H) pool to NADP(H) pool. They acknowledged that the activity of this transhydrogenase will consume energy, decreasing the yield. However, if reduction of acetoacetyl-CoA to R-3-hydroxybutyryl-CoA is driven by NADH, the activity of the energy consuming transhydrogenase is not necessary, and it would be possible to produce PHB as a fermentation product.



On the other hand, while different genes encoding for the enzymes required for the conversion of acetyl-CoA to PHB have been identified in many organisms, the successful expression in *E. coli* of the *phaCAB* operon from *Cupriavidus necator* (4) opened the way to tens of research projects focused on engineering the PHB accumulation. Given the cofactor preference of the acetoacetyl-CoA reductase from *C. necator* (AAR<sup>Cn</sup>), the reduction of acetoacetyl-CoA to R-3-hydroxybutyryl-CoA using such enzyme is coupled to NADPH consumption. An NADPH-consuming PHB production pathway implies competition for NADPH between PHB and biomass formations. Under these circumstances, the best growers are also the worst producers, leading to instability in the production strain. To avoid this problem, nitrogen-poor media are frequently employed to hinder biomass formation. Nonetheless, this approach affects protein and nucleotide synthesis, compromising the bio-conversion global rate (5).

Previous publications reported the use of NADH-preferring acetoacetyl-CoA reductases from *Allochromatium vinosum* and *Halomonas bluephagenesis* for PHB accumulation (6,7).

However, in those studies the cofactor preference was evaluated through a comparison between activities obtained at a single substrate and a single cofactor concentration.

Moreover, product inhibition by NAD<sup>+</sup> and NADP<sup>+</sup> were not evaluated, and saturation constants were not reported. Considering that, *in vivo*, NADPH/NADP<sup>+</sup> and NADH/NAD<sup>+</sup> ratios are different (8) and that these ratios change depending on physiological conditions (9,10), the assessment of the cofactor preference of any acetoacetyl-CoA reductase should be evaluated at physiologically meaningful NADPH/NADP<sup>+</sup> and NADH/NAD<sup>+</sup> ratios.

Therefore, the information provided in those previous reports is not enough to ensure the use of NADH over NADPH under physiological conditions.

Looking for an NADH-preferring acetoacetyl-CoA reductase engaged in PHB accumulation, we decided to study the enzyme from the bacterium *Candidatus Accumulibacter phosphatis* ( $AAR^{CAp}$ ). The choice of this organism was based on the following observations. First, this organism is able to anaerobically convert acetate and glucose equivalents into PHB with full electron conservation (Figure 1C). Therefore, it naturally does what Carlson and co-workers found as the ideal scenario for anaerobic PHB accumulation. Second, genomic and transcriptomic data indicate that this organism lacks the enzymes catalyzing the reactions of the oxidative branch of pentose-phosphate pathway (11), a common source of NADPH. Furthermore, no gene encoding for an  $NADP^+$ -depending non-phosphorylating glyceraldehyde-3-phosphate dehydrogenase was found in this bacterium. Therefore, oxidation of glucose equivalents should yield NADH. Third, if  $AAR^{CAp}$  is an NADPH-preferring enzyme, electrons derived from glucose equivalents oxidation (carried as NADH) must be transferred to NADPH by some transhydrogenase mechanism. Given the redox potential of NAD(H) and  $NADP(H)$  pools, transfer of reducing equivalents from the former to the latter pool requires energy (12,13). A more parsimonious and energetically cheaper solution is to have an NADH-preferring acetoacetyl-CoA reductase.

In the genome-scale metabolic network of *Ca. A. phosphatis* derived from meta-genomics data,  $AAR^{CAp}$  was annotated as an NADPH-preferring enzyme (14). Nevertheless, to the best of our knowledge, the kinetic properties of  $AAR^{CAp}$  have not yet been characterized. The direct use of NADH to drive the reduction of acetoacetyl-CoA to R-3-hydroxybutyryl-CoA has basic and applied implications. From the basic science perspective, it would mean that *Ca. A. phosphatis* developed a mechanism to transfer electrons from glycolysis to PHB accumulation without involving an energy-consuming transhydrogenase. From the applied

science perspective, it would mean that PHB can be produced as a fermentation product, avoiding competition for NADPH between biomass and PHB accumulation.

Aiming to find a *bona fide* NADH-preferring acetoacetyl-CoA reductase suitable for PHB accumulation, we characterized here the cofactor preference of an acetoacetyl-CoA reductase obtained from a *Ca. A. phosphatis*-enriched mixed culture. Moreover, we investigated the role of some key residues in the cofactor discrimination and we observed engagement of this enzyme in PHB accumulation.

## **2. Material and Methods**

### *2.1 DNA manipulations and strain construction*

All the steps for the construction of the several plasmids and strains employed in this research are detailed in Supplementary Material 1. Relevant information about the strains, primers and plasmids employed in this research are in the Supplementary Table 1, Supplementary Table 2 and Supplementary Table 3. DNA sequence maps of all the constructed plasmids can be found in the open access repository “NADH-driven polyhydroxybutyrate accumulation in *E. coli* dataset 2” available at Mendeley data. The access link is: <http://dx.doi.org/10.17632/954dxdncrv.1>

### *2.2 Cell-free extracts preparation*

Cells from *Ca. A. phosphatis* were obtained from a *Ca. A. phosphatis*-enriched mixed culture. This *Ca. A. phosphatis*-enriched culture was prepared as described by Smolders and co-

workers (15). In the case of *E. coli*, for all the here-studied strains, cells from previously isolated colonies were inoculated in Lysogenic Broth and aerobically grown for 16 hours at 37 °C, in an orbital shaker at 180 rpm. Ampicillin (100 µg/mL) or Kanamycin (30 µg/mL) was added, when required, to select cells carrying plasmids. Cultures had an optical density at 600 nm between 2.0 and 3.0 when cells were collected.

Broth samples (approx. 10 mL) were collected from *E. coli* cultures and the bioreactor containing cells of *Ca. A. phosphatis*. These samples were centrifuged (2500x g, 10 min, 4 °C) and extracellular media were discarded. Pellets were re-suspended in 10 mL of Buffer A (50 mM Tris (pH 8), 5 mM MgCl<sub>2</sub>, 5 mM NaCl). Cellular suspensions were centrifuged again (2500x g, 10 min, 4 °C) and supernatants were discarded. After this second centrifugation step, pellets were re-suspended in 10 mL of Buffer A supplemented with 2 mM (L+D) 1,4-dithiothreitol (DTT) and cOmplete™ protease inhibitor cocktail (Roche), following manufacturer's instructions. Cells were disrupted by sonication in an Ultrasonics™ S-250A Analog Ultrasonic Cell Disruptor (Branson), with output power set at level three, 30 % duty cycle, for 3 minutes per sample. Cellular suspensions were kept on ice while being sonicated to avoid overheating and protein denaturation. The resulting cellular suspensions were centrifuged (15000x g, 45 min, 4 °C). The obtained cell-free extracts were used for enzymatic assays. The protein concentration in the cell-free extracts was determined using the Bradford protein assay reagent (Bio-Rad) and bovine serum albumin (Bio-Rad) as standard (16).

### *2.3 Enzyme purification and characterization*

For over-expression of poly-histidine-tagged forms of the proteins encoded by *phaB*<sup>CAp6</sup>, *phaB*<sup>Cnecator</sup> and *phaB*<sup>Chimera</sup>, the plasmids pCOLA-His-*phaB*<sup>CAp6</sup>, pCOLA-His-*phaB*<sup>Cnecator</sup> and pCOLA-His-*phaB*<sup>Chimera</sup> were introduced in BL21(DE3) cells. Protein purification was achieved following a method previously described (17). Purity of the protein preparations (over 95 %) was assessed by SDS-PAGE.

The substrates employed for enzymatic assays were purchased from Sigma ((L+D) 3-hydroxybutyryl-CoA, NAD<sup>+</sup>, NADP<sup>+</sup>, NADH and NADPH) and Santa Cruz Biotechnology (acetoacetyl-CoA) and all had analytical grade quality. NADH and NADPH were freshly prepared by dissolving them in Buffer A. Acetoacetyl-CoA, NAD<sup>+</sup> and NADP<sup>+</sup> were freshly dissolved in des-ionized water (resistivity 18.2 MΩ\*cm at 25 °C). Substrate concentration in these stock solutions was estimated by spectrophotometry, dissolving samples taken from the stocks in 50 mM MOPS (pH 7), 5 mM MgCl<sub>2</sub>, 5 mM NaCl. The reactions were monitored in Buffer A at 30 °C. All the kinetic assays were performed in a Synergy HTX plate reader (Biotek), using path length correction. While some reactions were monitored at 310 nm to detect small changes in acetyl-CoA concentration, others were monitored at 360 nm to avoid absorbance values above 2.0 leading to the optical artefact known as “stray light” (18). To calculate acetoacetyl-CoA reductase activity, it was considered that, during the reactions, both acetoacetyl-CoA and NAD(P)H are consumed with a stoichiometric ratio 1:1. The apparent molar extinction coefficients were  $\epsilon^{\text{AcAcCoA},310} = 11000 \text{ M}^{-1} \text{ cm}^{-1}$  (19),  $\epsilon^{\text{NAD(P)H},310} = 3340 \text{ M}^{-1} \text{ cm}^{-1}$ ,  $\epsilon^{\text{AcAcCoA},360} = 900 \text{ M}^{-1} \text{ cm}^{-1}$  (19), and  $\epsilon^{\text{NAD(P)H},360} = 4275 \text{ M}^{-1} \text{ cm}^{-1}$ . The enzyme concentration in working stocks was determined using the Bradford protein assay reagent (Bio-Rad) and bovine serum albumin (Bio-Rad) as standard (16).

Some kinetic parameters were assessed through analyses of reaction progress curves while other were obtained studying the initial rates at different substrate concentrations. To

estimate initial rates, pseudo-linear temporal changes in absorbance were considered within time frames during which less than 5 % of the initial substrate had been consumed. Enzyme stability was evaluated with the test described by Selwyn (20). Global fitting of reaction progress curves to different mechanisms was evaluated by a model discrimination algorithm included in the software DYNAFIT (Biokin, version 4.08.137) (21). Raw kinetic data and DYNAFIT scripts are in the open access repository “NADH-driven polyhydroxybutyrate accumulation in *E. coli* dataset 2” available at Mendeley data.

#### *2.4 Protein structure analysis*

For homology modeling of AAR<sup>CAP</sup>, the X-ray crystal structure of a putative acetoacetyl-CoA reductase from *Burkholderia cenocepacia* bound to NADP<sup>+</sup> (PDB ID: 4K6F) was used as template. In the asymmetric unit, NADP<sup>+</sup> ligand was present at two active sites of the tetramer. In order to model the presence of NAD<sup>+</sup> in the AAR<sup>CAP</sup> active site, we deleted the atomic coordinates of the 2'-phosphate group of NADP<sup>+</sup> in 4K6F. Modeling was performed using Modeller (22) with NAD<sup>+</sup> as fixed ligand. Fifty models were created and ranked according to the Discrete Optimized Protein Energy (DOPE) score. The final model was subjected to energy minimization using the YASARA web server (23). The software VMD (24) was used to visualize structures and Multiseq analysis environment (25) was used for structural superposition.

#### *2.5 Continuous culture*

Setup and operation of the continuous culture was as previously described (26). Dilution rate was fixed to  $0.1 \text{ h}^{-1}$ . Cellular PHB content was measured by Isotope dilution mass spectrometry (IDMS), using the method described by Velasco Alvarez and co-workers (27). Details about medium composition; control of temperature, pH, dissolved oxygen; quantification of biomass concentration; quantification of organic compounds and PHB quantification can be found in Supplementary Material 4. Biomass composition ( $\text{C}_1\text{H}_{1.6749}\text{N}_{0.255}\text{O}_{0.3453}\text{S}_{0.0069}\text{P}_{0.0063}$ ;  $M_{\text{wx}} = 23.184 \text{ gCDW/CmolX}$ ; Reduction degree = 4.292) considered plasmid and heterologous protein burden. The unbalanced experimentally assessed rates, together with their associated errors, were the input to calculate reconciled rates, consistent with the mass and electron conservation laws.

### 3. Results and Discussion

#### *3.1 Cells from a Ca. A. phosphatis-enriched mixed culture showed a high NADH-dependent acetoacetyl-CoA reductase activity*

Use of NADH or NADPH for the reduction of acetoacetyl-CoA was observed first in a cell-free extract from a *Ca. A. phosphatis*-enriched mixed culture. Cell-free extracts obtained from *E. coli* K-12 MG1655 cultures, with or without the plasmid pBBRMCS-2-*phaCAB*<sup>Cnecator</sup>, were employed as controls. Given the kinetic parameters of the  $\text{AAR}^{\text{Cn}}$  ( $K_M^{\text{AcAcCoA(NADPH)}} = 9 \mu\text{M}$ ,  $K_M^{\text{NADPH}} = 19 \mu\text{M}$  (28)), the conditions of the assay (acetoacetyl-CoA  $200 \mu\text{M}$ , NADPH  $200 \mu\text{M}$ ) should be saturating for this enzyme.

As expected, the cell-free extract from *E. coli* cells expressing the *phaCAB* genes from *C. necator* showed a higher acetoacetyl-CoA reductase activity with NADPH than with NADH

(Table 1). However, in the cell-free extract from the *Ca. A. phosphatis*-enriched mixed culture, activity using NADH was 60 times higher than activity with NADPH. Moreover, this NADH-dependent activity was four times higher than the NADPH-dependent activity observed in the cell-free extract from *E. coli* cells carrying several episomal copies of the *phaCAB* genes from *C. necator* per cell. These results suggested that (i) acetoacetyl-CoA reductase is expressed at high levels in *Ca. A. phosphatis* and (ii) AAR<sup>CAP</sup> should prefer NADH instead of NADPH. However, we considered that to endorse the claiming of NADH preference, it was necessary to explore the kinetic behavior of the purified enzyme in a wider range of substrate and cofactor concentrations, and explore the strength of product inhibition.

### *3.2 The cloned phaB gene encodes for an NADH-preferring acetoacetyl-CoA reductase*

Using primers targeting the amino acid encoding sequence of the gene named CAP2UW1\_3919 in KEGG database (GenBank: [ACV37169.1](#)) and metagenomic DNA obtained from the *Ca. A. phosphatis*-enriched mixed culture, three slightly different nucleotide sequences were obtained from four sequenced clones (Supplementary Material 1, Supplementary Figure 1). Most of the differences in DNA sequences did not result in changes in the encoded amino acids. None of these sequences matched 100 % with the reference sequence CAP2UW1\_3919. Therefore, it is possible that the cloned genes do not correspond to the same species whose genome was previously assembled and annotated. It had been impossible to isolate colonies of *Ca. A. phosphatis* so far, and it is likely that different closely related species are grouped under this taxonomic name. However, amino acid identity was over 93 % in all the sequenced clones. Moreover, the residues D94, K99, Y185, Q147 and



Q150, identified as key residues for the enzymatic activity in AAR<sup>Cn</sup> (29), were conserved in the cloned sequences. Therefore, we considered those cloned genes as *phaB* homologues. Because the biological meaning of the observed DNA and protein polymorphism is not clear, for further characterization we chose the clone with the highest identity respect to the reference sequence: *phaB*<sup>CAP6</sup> (89 % DNA identity, 95 % amino acid identity). A group of amino acids relevant for cofactor specificity (see Section 3.3) in *phaB*<sup>CAP6</sup> was identical to the reference protein sequence.

Initial rates using purified enzyme showed that the protein encoded by *phaB*<sup>CAP6</sup> was able to catalyze the reduction of acetoacetyl-CoA, using both NADH and NADPH, but with very different rates ( $14 \pm 2 \mu\text{mol} \cdot \text{min}^{-1} \cdot \text{mg}^{-1}$  and  $0.07 \pm 0.02 \mu\text{mol} \cdot \text{min}^{-1} \cdot \text{mg}^{-1}$  respectively, acetoacetyl-CoA 100  $\mu\text{M}$ , NAD(P)H 100  $\mu\text{M}$ ). On the other hand, the enzyme was also able to catalyze the oxidation of (L+D)-3-hydroxybutyryl-CoA (100  $\mu\text{M}$ ) using NAD<sup>+</sup> (1 mM) as cofactor ( $0.61 \pm 0.01 \mu\text{mol} \cdot \text{min}^{-1} \cdot \text{mg}^{-1}$ ). However, no oxidation of (L+D)-3-hydroxybutyryl-CoA was detected when using NADP<sup>+</sup> (1 mM) as cofactor. Because (L+D)-3-hydroxybutyryl-CoA is a mix of two isomers, these results did not enable to discriminate the stereo-isomery of the product(s) generated during acetoacetyl-CoA reduction. Nevertheless, they are consistent with the NADH- and NADPH-linked activities registered in the cell-free extract from the *Ca. A. phosphatis*-enriched culture. Therefore, given the high DNA and amino acid identities, and the observed enzymatic activities, we considered the purified enzyme an acetoacetyl-CoA reductase from *Ca. A. phosphatis* (AAR<sup>CAP</sup>).

Analyses of progress curves from reactions with different initial concentrations of NADH or NADPH, and initial concentration of acetoacetyl-CoA (400  $\mu\text{M}$ ) fixed, were performed to estimate some kinetic parameters. The same approach was employed to study cases where initial acetoacetyl-CoA concentration was varying and initial NADPH concentration was fixed

(300  $\mu\text{M}$ ). Nevertheless, when acetoacetyl-CoA concentration varied while keeping fixed initial NADH concentration, we observed non-regular oscillations in the absorbance. Keeping in mind that substrate inhibition at different concentrations of NADH has been reported for other homologues (28,30-32), we tested different initial concentrations of NADH, but we did not find a way to prevent these oscillations. Therefore, in this specific case, kinetic parameters were obtained fitting the initial rates versus acetoacetyl-CoA concentration data to the simple Michaelis–Menten model, keeping initial NADH concentration fixed at 300  $\mu\text{M}$ . In the conditions chosen for the enzymatic assays, partial enzyme inactivation was observed when enzyme concentration was below 1 nM. Therefore, enzyme inactivation was considered when fitting progress curves data.

A compilation of the obtained kinetic parameters is presented in Table 2. The physical meaning of  $K_M$  parameters depends on the model employed to fit the related experimental data. The estimates of  $K_M^{\text{AcAcCoA}}$  and  $k_{cat}^{\text{AcAcCoA}}$  using NADH were obtained using the rapid-equilibrium model. The other kinetic parameters were obtained using the steady-state (Briggs-Haldane) approach. As expected, the turnover constants ( $k_{cat}$ ) for each cofactor were very similar, either when obtained varying the concentrations of substrate or cofactor (Table 2).

The individual analysis of the kinetic parameters enabled a first-sight comparison of the performances of AAR<sup>CAp</sup> using NADH or NADPH. Using NADH,  $K_M$  of both substrate and cofactor were lower,  $k_{cat}$  was higher, and  $\text{NAD}^+$  inhibited the rates less than  $\text{NADP}^+$ . Cofactor preference is often expressed as the ratio between the catalytic efficiencies ( $k_{cat}/K_M$ ) estimated for each cofactor. A comparison between the acetoacetyl-CoA reductases that had been kinetically characterized showed that AAR<sup>CAp</sup> has the lowest  $k_{cat}/K_M$  for NADPH and the second highest  $k_{cat}/K_M$  for NADH, only after the homologue from *Halomonas boliviensis*

(see Supplementary Table 4). However, the  $k_{cat}/K_M$  for NADPH of the acetoacetyl-CoA reductase from *H. boliviensis* is almost three times higher than its  $k_{cat}/K_M$  for NADH.

Therefore, according to such criterion, the acetoacetyl-CoA reductase from *H. boliviensis* is not a NADH-preferring enzyme.

Anyways, it is important to highlight that, for multi-substrates reactions, the comparison between the  $k_{cat}/K_M$  obtained with different substrates or cofactors reflects better the preference when the concentration of the co-substrate is saturating, a situation not necessarily occurring under physiological conditions. In our specific case, the low  $K_{ic}^{NAD(P)}$  values indicate that *in vivo* AAR<sup>CAp</sup> activity should be highly dependent on NAD(P) concentration and, therefore, on NAD(P)H/NAD(P) ratios. Because these ratios depend on the physiological conditions, cofactor preference is a dynamic property rather than a static number. For the calculation of this dynamic preference, we implemented a quantitative approach considering the variation of NAD<sup>+</sup>, NADP<sup>+</sup>, NADH, and NADPH concentrations inside physiologically feasible ranges.

For our quantitative approach, we applied the generic BiBi rate equation proposed by Rohwer and co-workers (33). Using this generic equation, the rate of NADH consumption in the reaction catalyzed by AAR<sup>CAp</sup> can be written as:

$$v^{NADH} = \frac{k_{cat}^{NADH} * E * \frac{NADH * AcAcCoA}{K^{NADH} * K^{AcAcCoA}} * \left(1 - \frac{NAD * 3HBCoA}{NADH * AcAcCoA * K_{eq}}\right)}{\left(1 + \frac{NADH}{K^{NADH}} + \frac{3HBCoA}{K^{3HBCoA}}\right) * \left(1 + \frac{AcAcCoA}{K^{AcAcCoA}} + \frac{NAD}{K^{NAD}}\right)}$$

where  $K^{NADH}$ ,  $K^{AcAcCoA}$ ,  $K^{3HBCoA}$  and  $K^{NAD}$  are dissociation constants associated to the interactions between the corresponding ligands and different forms of the enzyme.

However, *in vivo*, NAD<sup>+</sup> and NADH binding will be affected by NADP<sup>+</sup> and NADPH

concentrations because they can also bind to the enzyme. Considering NADPH and NADP<sup>+</sup> as competitive inhibitors of NADH and NAD<sup>+</sup> binding, the terms  $\overline{K^{NADH}}$  and  $\overline{K^{NAD}}$  were multiplied by the factor  $(1 + \text{NADPH}/K^{NADPH} + \text{NADP}/K^{NADP})$ . After introducing such modifications, the equation was written as:

$$v^{NADH} = \frac{k_{cat}^{NADH} * E * \frac{NADH * AcAcCoA}{K^{NADH} * (1 + \frac{NADPH}{K^{NADPH}} + \frac{NADP}{K^{NADP}})} * K_{NADH}^{AcAcCoA} * \left(1 - \frac{NAD * 3HBCoA}{NADH * AcAcCoA * K_{eq}}\right)}{\left(1 + \frac{NADH}{K^{NADH} * (1 + \frac{NADPH}{K^{NADPH}} + \frac{NADP}{K^{NADP}})} + \frac{3HBCoA}{K_{NADH}^{3HBCoA}}\right) * \left(1 + \frac{AcAcCoA}{K_{NADH}^{AcAcCoA}} + \frac{NAD}{K^{NAD} * (1 + \frac{NADPH}{K^{NADPH}} + \frac{NADP}{K^{NADP}})}\right)}$$

Clearly, it was possible to write a homologue equation describing the rate of NADPH consumption. Considering the experimentally determined  $K_M$  and  $K_{ic}$  as good approximations of the dissociation constants of the generic equation, the parameters  $\overline{k_{cat}^{NADH}}$ ,  $\overline{k_{cat}^{NADPH}}$ ,  $\overline{K^{NADH}}$ ,  $\overline{K^{NADPH}}$ ,  $\overline{K_{NADH}^{AcAcCoA}}$ ,  $\overline{K_{NADPH}^{AcAcCoA}}$ ,  $\overline{K^{NAD}}$  and  $\overline{K^{NADP}}$  were immediately available. The parameter  $\overline{K_{NADH}^{3HBCoA}}$  was not experimentally determined but it was estimated taking advantage of the Haldane relationship:

$$\overline{K_{NADH}^{3HBCoA}} = \frac{K_{eq} * k_{cat}^{reverse} * K^{NADH} * K_M^{AcAcCoA}}{k_{cat}^{forward} * K^{NAD}}$$

where  $\overline{k_{cat}^{reverse}}$  was calculated from the relationship between the  $V^{max}$  of the forward ( $14 \pm 2 \mu\text{mol} * \text{min}^{-1} * \text{mg}^{-1}$ ) and the backward ( $0.61 \pm 0.01 \mu\text{mol} * \text{min}^{-1} * \text{mg}^{-1}$ ) reactions, measured with purified enzyme:

$$\overline{k_{cat}^{reverse}} = \frac{0.61 * k_{cat}^{forward}}{14}$$

The value  $\overline{K_{eq}} = 92$  was obtained from literature (34). Although this latter value was estimated for reactions using NADPH, according to calculations using Equilibrator (35),  $\overline{K_{eq}}$  does not vary significantly after substituting NADP(H) by NAD(H). This way,  $\overline{K_{NADH}^{3HBCoA}} = 32 \mu\text{M}$  was calculated. This value is very similar to  $\overline{K_M^{3HBCoA}} = 33 \mu\text{M}$  estimated by Haywood and co-workers while studying the acetoacetyl-CoA reductase from *C. necator* (28). Making a similar assumption for the reaction using NADP(H),  $\overline{K_{NADPH}^{3HBCoA}} = 44300 \mu\text{M}$  was calculated.

However, beyond the availability of the required kinetic parameters, to obtain a physiologically meaningful result, it is important to evaluate the rate expressions with physiologically feasible substrate, product and cofactors concentrations. Because their ability of binding to other bio-molecules, free NAD(P)(H) concentrations are difficult to measure, and many experimentally reported values represent thermodynamically unfeasible states, as demonstrated by Canelas and co-workers (36). To overcome these problems, we calculated cofactor concentration ranges consistent with the thermodynamic constraints enabling the operation of glycolysis (37,38). In the case of NADH / NAD<sup>+</sup> ratios, it is known that these values depend on the redox potential of the available electron acceptor (9). This way, we explored NADH / NAD<sup>+</sup> ratios in the range between 0.03 (fully aerobic) and 0.71 (no external electron acceptor), according to experimentally determined values (9). Regarding the NADPH / NADP<sup>+</sup> ratios, there is a wide range of reported values in literature, from 0.32 (39) to 60 (40). Total moieties sizes of (NAD<sup>+</sup> + NADH) = 1470 + 100 = 1570  $\mu\text{M}$  and (NADP<sup>+</sup> + NADPH) = 195 + 62 = 257  $\mu\text{M}$  were considered, according to the data from Chassagnole and co-workers (39). Therefore, to calculate the ranges of individual cofactors concentrations, the following systems of simple algebraic equations were solved:

	NAD(H)	NADP(H)
More oxidized moiety	$\frac{NADH}{NAD} = 0.03$ (I) $NAD + NADH = 1570$ (II) Solutions: NAD = 1524 $\mu$ M; NADH = 46 $\mu$ M	$\frac{NADPH}{NADP} = 0.32$ (I) $NADP + NADPH = 257$ (II) Solutions: NADP = 195 $\mu$ M; NADPH = 62 $\mu$ M
More reduced moiety	$\frac{NADH}{NAD} = 0.71$ (I) $NAD + NADH = 1570$ (II) Solutions: NAD = 918 $\mu$ M; NADH = 652 $\mu$ M	$\frac{NADPH}{NADP} = 60$ (I) $NADP + NADPH = 257$ (II) Solutions: NADP = 4 $\mu$ M; NADPH = 253 $\mu$ M

Regarding acetoacetyl-CoA concentration, the equilibrium constant of the reaction catalyzed by the thiolase (E.C. 2.3.1.9),  $\overline{K_{eq}} = 1.1 \pm 0.2 * 10^{-5}$  (41) indicates that cytoplasmic acetoacetyl-CoA concentrations must be very low for the operation of this reaction in the forward direction. For example, considering acetyl-CoA and coenzyme A concentrations reported by Bennett and co-workers (40) (610 and 1400  $\mu$ M respectively), acetoacetyl-CoA concentration must be 0.03  $\mu$ M or lower. However, such a low concentration would represent a kinetic problem for the reaction catalyzed by AAR<sup>Cap</sup>. The existence of substrate channeling between the enzymes thiolase and acetoacetyl-CoA reductase could be a solution for this problem. Indeed, evidence of substrate channeling between these enzymes had been recently found (42,43). To overcome this uncertainty, for our calculations we assumed an acetoacetyl-CoA concentration of 22  $\mu$ M, as reported by Bennett and co-workers.

At the same time, the term  $(1 - ((NAD * 3HBCoA) / (NADH * AcAcCoA * K_{eq})))$  in the rate equation describing NADH consumption must be higher than 1, otherwise the reaction occurs in the backward direction. Using this term, it is possible to calculate the maximal R-3-

hydroxybutyryl-CoA concentration, corresponding to a situation of thermodynamic equilibrium:

$$\beta\text{HBCoA}^{max} = \frac{\text{NADH} * \text{AcAcCoA} * K_{eq}}{\text{NAD}}$$

In the more extreme case (fully aerobic conditions,  $\text{NADH}/\text{NAD}^+ = 0.03$ ), using the experimentally validated value of  $\sqrt{K_{eq}} = 92$  and an acetoacetyl-CoA concentration of  $22 \mu\text{M}$ :

$$\beta\text{HBCoA}^{max} = 0.03 * 22 \mu\text{M} * 92 = 61 \mu\text{M}$$

Given all these kinetic parameters, substrate, product and cofactors concentrations, it was possible to calculate the ratio  $R = v^{\text{NADH}}/v^{\text{NADPH}}$ , which indicates the relative use of NADH over NADPH by the enzyme  $\text{AAR}^{\text{CAp}}$ . According to this approach,  $\text{AAR}^{\text{CAp}}$  will have an R between 4 and 3975. It is important to notice that the relative use is independent of the enzyme concentration, as the terms E in the numerator and denominator of  $R = v^{\text{NADH}}/v^{\text{NADPH}}$  cancel each other.

As a way to validate this novel approach, we applied it to calculate the  $R = v^{\text{NADH}}/v^{\text{NADPH}}$  for the enzyme  $\text{AAR}^{\text{Cn}}$ , a well-documented NADPH-preferring homologue (28,44). As expected, the resulting analysis showed that  $\text{AAR}^{\text{Cn}}$  has a preference for NADPH over NADH between 17 and 33136. The relative use of NADH over NADPH (or vice versa) by  $\text{AAR}^{\text{CAp}}$  and  $\text{AAR}^{\text{Cn}}$  at physiological  $\text{NADPH}/\text{NADP}^+$  and  $\text{NADH}/\text{NAD}^+$  ratios is presented in Figure 2.

It was not possible to calculate the relative use of NADH and NADPH by the acetoacetyl-CoA reductases from *H. bluephagenesis* and *A. vinosum*, either comparing the  $k_{cat}/K_M$  for NADH and NADPH or using the above described approach because the required kinetic parameters are not available. In the case of *H. bluephagenesis*, the values  $k_{cat}^{\text{NADH}} = 72 \text{ s}^{-1}$  and  $k_{cat}^{\text{NADPH}} = 31 \text{ s}^{-1}$  can be calculated from the reported maximum velocities and the molecular weight of the monomer (7). However, no saturation constants were reported.

Summarizing, our kinetic analyses show that (i) at physiological concentrations, AAR<sup>CAp</sup> will largely prefer NADH over NADPH and (ii) AAR<sup>CAp</sup> is the acetoacetyl-CoA reductase with the highest preference for NADH among the homologues that have been kinetically characterized so far.

### *3.3 The residues between E37 and P41 have an important role in the observed cofactor specificity*

Previous studies tried to identify which are the structural determinants of the cofactor preference observed in some acetoacetyl-CoA reductases. De las Heras and co-workers suggested (i) the absence of the R40 residue present in the NADPH-preferring AAR<sup>Cn</sup> and (ii) the presence of the acidic E37 residue as the key determinants of the use of NADH by the acetoacetyl-CoA reductase from *A. vinosum* (6). On the other hand, Chen and co-workers pointed to (i) the substitution of the G35, S38 and R40 (according to residue numeration in AAR<sup>Cn</sup>) by other residues and (ii) the presence of the acidic E40 residue (aligned with the E37 of the acetoacetyl-CoA reductase from *A. vinosum*) as the key determinants for the use of NADH by the acetoacetyl-CoA reductase from *H. bluephagenesis* (7). However, these hypotheses were not experimentally tested. AAR<sup>CAp</sup> also has the E37 residue but comparing the NADH- and the NADPH-linked acetoacetyl-CoA reductase specific activities recorded in cell-free extracts, the ratio 720/11  $\approx$  65 observed in the *Ca. A. phosphatis*-enriched culture is a value higher than the ratio 56/5  $\approx$  24 observed in *H. bluephagenesis* (7) or the ratio 185/39  $\approx$  5 observed in the yeasts expressing the acetoacetyl-CoA reductase from *A. vinosum* (6). Therefore, we reasoned that other structural determinants should have a role in the cofactor discrimination in AAR<sup>CAp</sup>.



Looking for a deeper understanding of the interactions determining the high selectivity toward NADH observed in AAR<sup>CAP</sup>, we carried out a homology modeling, using the structure from *Burkholderia cenocepacia* as template. The choice of this species to guide the generation of the homology model is supported by the fact of *B. cenocepacia* being the closest species where a tridimensional structure of an acetoacetyl-CoA reductase complexed with a cofactor is available (Supplementary Material 2). Since both the K40 residue observed in AAR<sup>CAP</sup> and the R40 residue in AAR<sup>Cn</sup> have a positively charged side-chain, making a simple alignment of primary structures, one might expect that AAR<sup>CAP</sup> should also prefer NADPH. However, the presence of a proline residue at the following position (P41) disrupts the  $\alpha$ -helix 2 structure such that the positively charged side-chain of K40 is moved away from the binding pocket (Figure 3). In addition, the bulky side-chain of the F38 residue present in AAR<sup>CAP</sup> could produce steric hindrance with the 2'-phosphate of NADPH. On the other hand, interactions with NADH are not impaired by these structural features. Therefore, the displacement of the positively charged side-chain of K40 in combination with the presence of the bulky side-chain of F38 should be key structural traits determining the preference for NADH observed in AAR<sup>CAP</sup>. Notably, this combination of structural features is not shared with other acetoacetyl-CoA reductases that reportedly can use NADH as substrate (Supplementary Figure 2).

To substantiate our hypothesis about the role of these residues in the observed cofactor specificity, we generated, by artificial synthesis, a gene encoding for a mutant enzyme. In this mutant enzyme, the original segment between the amino acids N37 and R41 of the NADPH-preferring AAR<sup>Cn</sup> was replaced by the corresponding amino acids from AAR<sup>CAP</sup> (E37 to P41). This mutant, named AAR<sup>Chimera</sup>, was cloned in the vector pCOLA-duet-1 and it was over-expressed in *E. coli* BL21(DE3) cells. For comparison, *E. coli* BL21(DE3) cells carrying the

empty plasmid pCOLA-duet-1, the plasmid pCOLA-phaB-Cnecator (enabling the over-expression of the parental AAR<sup>Cn</sup>) and the plasmid pCOLA-His-phaB<sup>CAp6</sup> were grown in parallel. Specific acetoacetyl-CoA reductase activities, using NADH and NADPH, were evaluated in cell-free extracts coming from these strains. The average NADH- and NADPH-linked activities recorded in the cell-free extract from the cells carrying the empty plasmid pCOLA-duet-1 were considered as background signals and subtracted to the activities obtained with the other extracts. The net NADH- and NADPH-linked activities recorded in the cell-free extracts strongly suggested that AAR<sup>Chimera</sup> has a cofactor preference somewhere between the parental NADPH-preferring AAR<sup>Cn</sup> and the NADH-preferring AAR<sup>CAp</sup> (Table 3).

AAR<sup>Chimera</sup> was purified, and reactions using NADH or NADPH as cofactor were kinetically characterized by progress curves analysis. The results obtained with purified enzyme are consistent with the data obtained with cell-free extracts (Table 3). For comparison, some kinetic parameters of the parental NADPH-preferring AAR<sup>Cn</sup> and the NADH-preferring AAR<sup>CAp</sup> were included. In the case of AAR<sup>Cn</sup>, kinetic parameters obtained with purified enzyme were found in the reports of Haywood and co-workers (28) and Matsumoto and co-workers (44). While Matsumoto and co-workers characterized the enzyme activity using only NADPH, Haywood and co-workers studied the activities with NADH and NADPH. Then, we chose the data reported by the latter to compare the cofactor preferences among AAR<sup>Cn</sup>, AAR<sup>Chimera</sup> and AAR<sup>CAp</sup> using the parameter  $(k_{cat}/K_M^{NADH}) / (k_{cat}/K_M^{NADPH})$  (Table 3). Despite the differences between the kinetic parameters reported by Haywood and co-workers and Matsumoto and co-workers, their estimates of  $(k_{cat}/K_M^{NADPH})$  are similar ( $2.62 \times 10^5 \text{ M}^{-1}\text{s}^{-1}$  and  $6.85 \times 10^5 \text{ M}^{-1}\text{s}^{-1}$ , respectively). Therefore, either comparing the observations from

Haywood and co-workers or Matsumoto and co-workers, our conclusion about the shift in cofactor specificity in AAR<sup>Chimera</sup> respect to the parental AAR<sup>Cn</sup> would be qualitatively similar. It was possible to observe that, in comparison with the parental AAR<sup>Cn</sup>, the modifications improved the performance using NADH while impaired the performance using NADPH (Table 3). Although a full reversion of the cofactor specificity of AAR<sup>Cn</sup> will require further modifications, our results endorse the proposed hypothesis regarding the role of the residues between E37 and P41 as structural determinants of the NADH preference observed for AAR<sup>CAp</sup>. Moreover, further understanding of the structural determinants in the dinucleotide binding pocket (Supplementary Material 2, Supplementary Figure 3) could be useful for genomic screenings looking for other putative NADH-preferring acetoacetyl-CoA reductases or could be valuable as starting point for further protein/metabolic engineering efforts.

### 3.4 AAR<sup>CAp</sup> can be engaged in PHB accumulation

To verify *in vivo* functionality of AAR<sup>CAp</sup>, an operon was assembled joining the *phaCA* genes from *C. necator* with the *phaB*<sup>CAp6</sup> gene; and this operon was placed under the control of T7 promoter. The resultant plasmid was introduced in *E. coli* MG1655(DE3) cells, which are able to express T7 RNA polymerase upon induction with IPTG (Supplementary Material 3). NADH-linked acetoacetyl-CoA reductase activity was observed, and this activity increased while increasing IPTG concentration in the medium (Supplementary Figure 4). Therefore, it was concluded that it was possible to regulate the expression of the genes *phaCA*<sup>Cnecator</sup> *phaB*<sup>CAp</sup> placed under the control of T7 promoter. Moreover, using the estimated kinetic parameters and the observed specific activity, it was possible to calculate the abundancy of AAR<sup>CAp</sup> and

the metabolic flux that such enzyme capacity can sustain (Supplementary Material 3).

According to such calculations, with the maximum observed specific activity (11 nmol/min/mg), it should be possible to sustain a maximum flux around 0.08 mmol/gCDW/h (Supplementary Figure 5).

However, the observation of NADH-linked acetoacetyl-CoA reductase activity does not necessarily guarantee the expression of other genes placed in the same operon nor an *in vivo* operative PHB pathway. Therefore, we next sought to link the accumulation of PHB in *E. coli* to the presence of the operon *phaCA*<sup>Cnecator</sup>*phaB*<sup>CAp</sup> in order to provide evidence of (i) *in vivo* functionality of the operon *phaCA*<sup>Cnecator</sup>*phaB*<sup>CAp</sup> and (ii) the ability of AAR<sup>CAp</sup> to be engaged in an PHB accumulation process.

Aiming a more accurate tracking of the carbon and electrons in the system, we chose to study the PHB accumulation using a continuous culture. Given the clear preference for NADH of AAR<sup>CAp</sup>, we reasoned that a reduction in oxygen supply must lead to an increase in PHB accumulation, provided the generation of other fermentation products be reduced. To ensure a reduced/null generation of other fermentation products, *E. coli* MG1655(DE3)<sup>Δ5</sup> (F- $\lambda$ -*ilvG*-*rfb*-50 *rph*-1 (DE3)  $\Delta$ *adhE*  $\Delta$ *adhP*  $\Delta$ *ldhA*  $\Delta$ *pta*  $\Delta$ *mhpF*) was chosen as a suitable strain to express the operon *phaCA*<sup>Cnecator</sup>*phaB*<sup>CAp</sup>.

Given the relatively low acetoacetyl-CoA reductase activity observed in the cell-free extracts from *E. coli* cells expressing the operon *phaCA*<sup>Cnecator</sup>*phaB*<sup>CAp</sup> (Supplementary Figure 4) in comparison with the acetoacetyl-CoA reductase activity registered in the cell-free extract from the *Ca. A. phosphatis*-enriched mixed culture (Table 1), we decided to not integrate this operon in the chromosome. Nevertheless, to avoid the use of antibiotic during a continuous culture, the genes *cscABK* from *E. coli* W were introduced in the same plasmid already carrying the operon *phaCA*<sup>Cnecator</sup>*phaB*<sup>CAp</sup>, resulting the plasmid pCOLA-*phaCA*<sup>Cnecator</sup>*phaB*<sup>CAp</sup>-

cscABK. This way, the use of sucrose as the sole carbon source was the selection pressure to maintain the plasmid, as previously demonstrated (26).

The continuous growth of *E. coli* MG1655(DE3)<sup>Δ5</sup> transformed with the plasmid pCOLA-*phaCA*<sup>Cnecator</sup>*phaB*<sup>CAP</sup>-cscABK, using sucrose as the sole carbon source, was studied under oxygen limiting conditions, at a dilution rate of 0.1 h<sup>-1</sup>. To enable the expression of the operon *phaCA*<sup>Cnecator</sup>*phaB*<sup>CAP</sup>, the feeding solution was supplemented with IPTG (100 μM).

Being aware of previous reports of genetic instabilities when using episomal expression systems enabling the sucrose consumption (45), the presence of the plasmid pCOLA-*phaCA*<sup>Cnecator</sup>*phaB*<sup>CAP</sup>-cscABK was monitored by colony-PCR. In our conditions, no plasmid loss was verified (data not shown).

Two steady-states, characterized by different levels of oxygen limitation, were characterized (Table 4). Aiming to achieve a stable oxygen consumption rate below 2.9 mmol O<sub>2</sub>/gCDW/h, we tried to further decrease the oxygen supply while keeping the same dilution rate.

However, this attempt brought instabilities in off-gas composition that were not stabilized after ten residence times.

Given the inability of wild-type *E. coli* to produce PHB, the observed accumulation, *irrespective to the obtained PHB titers*, confirmed the ability of AAR<sup>CAP</sup> to be engaged in PHB accumulation and confirmed the *in vivo* functionality of the operon *phaCA*<sup>Cnecator</sup>*phaB*<sup>CAP</sup>.

Moreover, in the steady-state with the lowest oxygen consumption rate, PHB accumulation increased more than 30 times respect to the other steady-state (Table 4).

From a historical perspective, there are previous reports of increments in PHB accumulation linked to oxygen limitation in *Azotobacter beijerinckii* (46) and *Azotobacter vinelandii* (47).

One potential explanation for those observations was the use of NADH to drive PHB accumulation. However, kinetic characterizations of the acetoacetyl-CoA reductases present

in those bacteria showed that they prefer NADPH instead of NADH (34,48). In our case, the kinetic characterization clearly indicated that, in the physiological conditions, AAR<sup>CAP</sup> prefers NADH. Different to previous reports claiming NADH-driven accumulation of PHB using the acetoacetyl-CoA reductases from *A. vinosum* and *H. bluephagenesis*, we are endorsing our claiming with a kinetic analysis considering physiologically relevant and dynamic concentrations of NAD<sup>+</sup>, NADP<sup>+</sup>, NADH and NADPH.

Finally, according to several previous observations, *Ca. A. phosphatis* accumulates PHB in anaerobic conditions coupled to glycogen mobilization and acetate uptake. Different to *A. vinosum* or *H. bluephagenesis*, *Ca. A. phosphatis* does not have an NADPH-producing oxidative branch of the pentose-phosphate pathway. This way, the oxidation of glucose or glucose equivalents yields electrons carried only by NADH. Because PHB has a higher electron/carbon ratio than glucose, polymer accumulation could operate as a mechanism to re-oxidize NADH in such conditions. One way to enable this re-oxidation is having an NADH-preferring acetoacetyl-CoA reductase. Therefore, the NADH-preference of AAR<sup>CAP</sup> is consistent with the ecological and biochemical conditions present during PHB accumulation in *Ca. A. phosphatis*, highlighting the importance of a multi-disciplinary approach when looking for enzymes with different/new properties.

#### **4. Conclusions**

In this research, we identified and characterized an acetoacetyl-CoA reductase that prefers NADH over NADPH in a wide range of physiologically feasible NAD(P)(H) concentrations. Moreover, a structural analysis and further kinetic characterization of a mutant enzyme indicated a group of key amino acids with a relevant role in the observed cofactor specificity,

opening the way to further protein engineering approaches and to the quest for other NADH-specific acetoacetyl-CoA reductases in other (meta)genomes. Finally, evidence of engagement of this NADH-preferring acetoacetyl-CoA reductase in PHB accumulation was shown.

The identification of an NADH-preferring acetoacetyl-CoA reductase able to participate in PHB accumulation is a key piece to develop metabolic engineering strategies envisioning generation of PHB as a fermentation product. Yet, this piece alone does not solve the mismatch between catabolic supply and PHB formation demand of acetyl-CoA and electrons (Figure 1). Therefore, the substitution of the two sources of acetyl-CoA (external acetate and internal glycogen) present in *Ca. A. phosphatis* by a single external source, together with the removal of eventual energetic and kinetic bottlenecks, should be the focus of future metabolic engineering strategies envisioning anaerobic generation of PHB as a single/main fermentation product.

#### **Funding:**

This work was supported by the joint research program NWO–FAPESP of The Netherlands Organization for Scientific Research (NWO) and São Paulo Research Foundation (FAPESP) (NWO: BRAZIL.2013.018 – FAPESP: 2013/50357-2). The contributions of Karel Olavarria and M.C.M. van Loosdrecht were also supported by a SIAM Gravitation Grant (024.002.002) from the Netherlands Ministry of Education, Culture and Science (OCW) and NWO. The authors declare they do not have any potential conflict of interest.

## References

1. Lemoigne, M. (1926) Produits de dehydration et de polymerisation de l'acide  $\beta$ -oxobutyrique. *Bulletin de la Société de Chimie Biologique* **8**, 770-782
2. Cueto-Rojas, H. F., van Maris, A. J. A., Wahl, S. A., and Heijnen, J. J. (2015) Thermodynamics-based design of microbial cell factories for anaerobic product formation. *Trends in Biotechnology* **33**, 534-546
3. Carlson, R., Wlaschin, A., and Sreenc, F. (2005) Kinetic studies and biochemical pathway analysis of anaerobic poly-(R)-3-hydroxybutyric acid synthesis in *Escherichia coli*. *Appl Environ Microbiol* **71**, 713-720
4. Schubert, P., Steinbuchel, A., and Schlegel, H. G. (1988) Cloning of the *Alcaligenes eutrophus* genes for synthesis of poly-beta-hydroxybutyric acid (PHB) and synthesis of PHB in *Escherichia coli*. *J Bacteriol* **170**, 5837-5847
5. Chen, Z., Zhao, L., Ji, Y., Wen, Q., and Huang, L. (2019) Reconsideration on the effect of nitrogen on mixed culture polyhydroxyalkanoate production toward high organic loading enrichment history. *Frontiers of Environmental Science & Engineering* **13**, 54
6. de Las Heras, A. M., Portugal-Nunes, D. J., Rizza, N., Sandstrom, A. G., and Gorwa-Grauslund, M. F. (2016) Anaerobic poly-3-D-hydroxybutyrate production from xylose in recombinant *Saccharomyces cerevisiae* using a NADH-dependent acetoacetyl-CoA reductase. *Microb Cell Fact* **15**, 197
7. Ling, C., Qiao, G. Q., Shuai, B. W., Olavarria, K., Yin, J., Xiang, R. J., Song, K. N., Shen, Y. H., Guo, Y., and Chen, G. Q. (2018) Engineering NADH/NAD(+) ratio in *Halomonas* bluephagenesis for enhanced production of polyhydroxyalkanoates (PHA). *Metab Eng* **49**, 275-286
8. Andersen, K. B., and von Meyenburg, K. (1977) Charges of nicotinamide adenine nucleotides and adenylate energy charge as regulatory parameters of the metabolism in *Escherichia coli*. *J Biol Chem* **252**, 4151-4156



9. de Graef, M. R., Alexeeva, S., Snoep, J. L., and Teixeira de Mattos, M. J. (1999) The steady-state internal redox state (NADH/NAD) reflects the external redox state and is correlated with catabolic adaptation in *Escherichia coli*. *J Bacteriol* **181**, 2351-2357
10. Krapp, A. R., Victoria Humbert, M., and Carrillo, N. (2011) The soxRS response of *Escherichia coli* can be induced in the absence of oxidative stress and oxygen by modulation of NADPH content. *Microbiology-Sgm* **157**, 957-965
11. Garcia Martin, H., Ivanova, N., Kunin, V., Warnecke, F., Barry, K. W., McHardy, A. C., Yeates, C., He, S., Salamov, A. A., Szeto, E., Dalin, E., Putnam, N. H., Shapiro, H. J., Pangilinan, J. L., Rigoutsos, I., Kyrpides, N. C., Blackall, L. L., McMahon, K. D., and Hugenholtz, P. (2006) Metagenomic analysis of two enhanced biological phosphorus removal (EBPR) sludge communities. *Nat Biotechnol* **24**, 1263-1269
12. Reich, J. G., and Sel'kov, E. E. (1981) *Energy metabolism of the cell : a theoretical treatise*, Academic Press, London ; New York
13. Spaans, S. K., Weusthuis, R. A., van der Oost, J., and Kengen, S. W. (2015) NADPH-generating systems in bacteria and archaea. *Front Microbiol* **6**, 742
14. Oyserman, B. O., Noguera, D. R., del Rio, T. G., Tringe, S. G., and McMahon, K. D. (2016) Metatranscriptomic insights on gene expression and regulatory controls in *Candidatus Accumulibacter phosphatis*. *The ISME journal* **10**, 810-822
15. Smolders, G. J., van der Meij, J., van Loosdrecht, M. C., and Heijnen, J. J. (1994) Model of the anaerobic metabolism of the biological phosphorus removal process: Stoichiometry and pH influence. *Biotechnol Bioeng* **43**, 461-470
16. Bradford, M. M. (1976) A rapid and sensitive method for the quantitation of microgram quantities of protein utilizing the principle of protein-dye binding. *Anal Biochem* **72**, 248-254
17. Olavarria, K., Marone, M. P., da Costa Oliveira, H., Roncallo, J. C., da Costa Vasconcelos, F. N., da Silva, L. F., and Gomez, J. G. (2015) Quantifying NAD(P)H production in the upper Entner-Doudoroff pathway from *Pseudomonas putida* KT2440. *FEBS Open Bio* **5**, 908-915

18. Cavalieri, R. L., and Sable, H. Z. (1974) Pitfalls in the study of steady state kinetics of enzymes: spurious inhibition patterns due to stray light errors. *Anal Biochem* **59**, 122-128
19. Stern, J. R. (1956) Optical properties of aceto-acetyl-S-coenzyme A and its metal chelates. *J Biol Chem* **221**, 33-44
20. Selwyn, M. J. (1965) A simple test for inactivation of an enzyme during assay. *Biochim Biophys Acta* **105**, 193-195
21. Kuzmic, P. (1996) Program DYNAFIT for the analysis of enzyme kinetic data: Application to HIV proteinase. *Analytical Biochemistry* **237**, 260-273
22. Sali, A., and Blundell, T. L. (1993) Comparative protein modelling by satisfaction of spatial restraints. *J Mol Biol* **234**, 779-815
23. Krieger, E., Joo, K., Lee, J., Lee, J., Raman, S., Thompson, J., Tyka, M., Baker, D., and Karplus, K. (2009) Improving physical realism, stereochemistry, and side-chain accuracy in homology modeling: Four approaches that performed well in CASP8. *Proteins* **77 Suppl 9**, 114-122
24. Humphrey, W., Dalke, A., and Schulten, K. (1996) VMD: Visual molecular dynamics. *Journal of Molecular Graphics & Modelling* **14**, 33-38
25. Roberts, E., Eargle, J., Wright, D., and Luthey-Schulten, Z. (2006) MultiSeq: unifying sequence and structure data for evolutionary analysis. *BMC Bioinformatics* **7**, 382
26. Olavarria, K., Fina, A., Velasco, M. I., van Loosdrecht, M. C. M., and Wahl, S. A. (2019) Metabolism of sucrose in a non-fermentative Escherichia coli under oxygen limitation. *Applied Microbiology and Biotechnology*
27. Velasco Alvarez, M. I., Ten Pierick, A., van Dam, P. T. N., Maleki Seifar, R., van Loosdrecht, M. C. M., and Wahl, S. A. (2017) Microscale Quantitative Analysis of Polyhydroxybutyrate in Prokaryotes Using IDMS. *Metabolites* **7**
28. Haywood, G. W., Anderson, A. J., Chu, L., and Dawes, E. A. (1988) The role of NADH- and NADPH-linked acetoacetyl-CoA reductases in the poly-3-hydroxybutyrate synthesizing

organism *Alcaligenes eutrophus* FEMS Microbiology Letters Volume 52, Issue 3. *FEMS Microbiology Letters*

29. Kim, J., Chang, J. H., Kim, E. J., and Kim, K. J. (2014) Crystal structure of (R)-3-hydroxybutyryl-CoA dehydrogenase PhaB from *Ralstonia eutropha*. *Biochem Biophys Res Commun* **443**, 783-788
30. Fukui, T., Ito, M., Saito, T., and Tomita, K. (1987) Purification and characterization of NADP-linked acetoacetyl-CoA reductase from *Zoogloea ramigera* I-16-M. *Biochim Biophys Acta* **917**, 365-371
31. Ploux, O., Masamune, S., and Walsh, C. T. (1988) The NADPH-linked acetoacetyl-CoA reductase from *Zoogloea ramigera*. Characterization and mechanistic studies of the cloned enzyme over-produced in *Escherichia coli*. *Eur J Biochem* **174**, 177-182
32. Mothes, G., and Babel, W. (1994) *Methylobacterium rhodesianum* MB 126 possesses two acetoacetyl-CoA reductases. *Archives of Microbiology* **161**, 277-280
33. Rohwer, J. M., Hanekom, A. J., Crous, C., Snoep, J. L., and Hofmeyr, J. H. (2006) Evaluation of a simplified generic bi-substrate rate equation for computational systems biology. *Syst Biol (Stevenage)* **153**, 338-341
34. Ritchie, G. A., Senior, P. J., and Dawes, E. A. (1971) The purification and characterization of acetoacetyl-coenzyme A reductase from *Azotobacter beijerinckii*. *Biochem J* **121**, 309-316
35. Flamholz, A., Noor, E., Bar-Even, A., and Milo, R. (2012) eQuilibrator--the biochemical thermodynamics calculator. *Nucleic Acids Res* **40**, D770-775
36. Canelas, A. B., van Gulik, W. M., and Heijnen, J. J. (2008) Determination of the cytosolic free NAD/NADH ratio in *Saccharomyces cerevisiae* under steady-state and highly dynamic conditions. *Biotechnology and Bioengineering* **100**, 734-743
37. Kummel, A., Panke, S., and Heinemann, M. (2006) Putative regulatory sites unraveled by network-embedded thermodynamic analysis of metabolome data. *Mol Syst Biol* **2**, 2006.0034

38. Henry, C. S., Broadbelt, L. J., and Hatzimanikatis, V. (2007) Thermodynamics-based metabolic flux analysis. *Biophys J* **92**, 1792-1805
39. Chassagnole, C., Noisommit-Rizzi, N., Schmid, J. W., Mauch, K., and Reuss, M. (2002) Dynamic modeling of the central carbon metabolism of *Escherichia coli*. *Biotechnology and Bioengineering* **79**, 53-73
40. Bennett, B. D., Kimball, E. H., Gao, M., Osterhout, R., Van Dien, S. J., and Rabinowitz, J. D. (2009) Absolute metabolite concentrations and implied enzyme active site occupancy in *Escherichia coli*. *Nat Chem Biol* **5**, 593-599
41. Lan, E. I., and Liao, J. C. (2012) ATP drives direct photosynthetic production of 1-butanol in cyanobacteria. *Proc Natl Acad Sci U S A* **109**, 6018-6023
42. Tippmann, S., Anfelt, J., David, F., Rand, J. M., Siewers, V., Uhlén, M., Nielsen, J., and Hudson, E. P. (2017) Affibody Scaffolds Improve Sesquiterpene Production in *Saccharomyces cerevisiae*. *ACS Synth Biol* **6**, 19-28
43. Vögeli, B., Engilberge, S., Girard, E., Riobé, F., Maury, O., Erb, T. J., Shima, S., and Wagner, T. (2018) Archaeal acetoacetyl-CoA thiolase/HMG-CoA synthase complex channels the intermediate via a fused CoA-binding site. *Proc Natl Acad Sci U S A* **115**, 3380-3385
44. Matsumoto, K. i., Tanaka, Y., Watanabe, T., Motohashi, R., Ikeda, K., Tobitani, K., Yao, M., Tanaka, I., and Taguchi, S. (2013) Directed Evolution and Structural Analysis of NADPH-Dependent Acetoacetyl Coenzyme A (Acetoacetyl-CoA) Reductase from *Ralstonia eutropha* Reveals Two Mutations Responsible for Enhanced Kinetics. *Applied and environmental microbiology* **79**, 6134-6139
45. Bruschi, M., Boyes, S. J., Sugiarto, H., Nielsen, L. K., and Vickers, C. E. (2012) A transferable sucrose utilization approach for non-sucrose-utilizing *Escherichia coli* strains. *Biotechnol Adv* **30**, 1001-1010
46. Senior, P. J., Beech, G. A., Ritchie, G. A., and Dawes, E. A. (1972) The role of oxygen limitation in the formation of poly- $\gamma$ -hydroxybutyrate during batch and continuous culture of *Azotobacter beijerinckii*. *Biochem J* **128**, 1193-1201

47. Page, W. J., and Knosp, O. (1989) Hyperproduction of Poly-beta-Hydroxybutyrate during Exponential Growth of *Azotobacter vinelandii* UWD. *Appl Environ Microbiol* **55**, 1334-1339
48. Manchak, J., and Page, W. J. (1994) Control of polyhydroxyalkanoate synthesis in *Azotobacter vinelandii* strain UWD. *Microbiology* **140**, 953-963

Table 1: Specific AAR activities, using NADH or NADPH, in cell-free extracts from *E. coli* expressing the *phaCAB* genes from *C. necator* and from a *Ca. A. phosphatis*-enriched mixed culture

Biological sample	cofactor	mean $\pm$ SD (U/mg)
<i>E. coli</i> MG1655 + pBBRMCS-2- <i>phaCAB</i> <sup>Cnecator</sup>	NADH	0.026 $\pm$ 0.001
<i>E. coli</i> MG1655 + pBBRMCS-2- <i>phaCAB</i> <sup>Cnecator</sup>	NADPH	0.196 $\pm$ 0.021
<i>Ca. A. phosphatis</i> -enriched mixed culture	NADH	0.720 $\pm$ 0.094
<i>Ca. A. phosphatis</i> -enriched mixed culture	NADPH	0.011 $\pm$ 0.002

1 U/mg = 1  $\mu\text{mol} \cdot \text{min}^{-1}$  per milligram of cytoplasmic proteins

Table 2: Kinetic parameters observed for the purified AAR<sup>CAp</sup>. The best fitted values are accompanied by the 95 % confidence intervals (in parentheses). Acetoacetyl-CoA was abbreviated as AcAcCoA.

	NAD(H)	NADP(H)
$K_M$ ( $\mu\text{M}$ )	7.7 (6.74, 8.67)	44.3 (40.4, 48.5)
$k_{cat}$ ( $\text{s}^{-1}$ )	8.9 (8.8, 9.0)	0.09 (0.092, 0.098)
$K_{ic}^{\text{NAD(P)}}$ ( $\mu\text{M}$ )	54.5 (44.8, 66.0)	1.27 (1.19, 1.35)
$K_M^{\text{AcAcCoA}}$ ( $\mu\text{M}$ )	56.7 (42.7, 74.5)	318 (303, 334)
$k_{cat}^{\text{AcAcCoA}}$ ( $\text{s}^{-1}$ )	11.6 (10.5, 12.9)	0.131 (0.127, 0.136)





Table 3: Kinetic properties of acetoacetyl-CoA reductases with different cofactor preference.

	Data obtained with cell-free extracts <sup>(a)</sup>			Data obtained with purified enzymes				
	sp. activity NADH (U/mg)	sp. activity NADPH (U/mg)	Ratio sp. activities	$k_{cat}^{NADH}$ (s <sup>-1</sup> )	$K_M^{NADH}$ (μM)	$k_{cat}^{NADPH}$ (s <sup>-1</sup> )	$K_M^{NADPH}$ (μM)	$(k_{cat}/K_M^{NADH}) / (k_{cat}/K_M^{NADPH})$
AAR <sup>Cn</sup>	0.13 ± 0.07	0.68 ± 0.13	0.19	1.0 <sup>(b)</sup>	400 <sup>(b)</sup>	5 <sup>(b)</sup>	19 <sup>(b)</sup>	0.01
AAR <sup>Chimera</sup>	0.93 ± 0.18	0.29 ± 0.07	3.18	5.14 ± 0.03	77 ± 3	9.30 ± 0.05	665 ± 6	4.75
AAR <sup>CAP</sup>	1.96 ± 0.11	0.25 ± 0.03	7.88	8.92 ± 0.05	7.7 ± 0.5	0.095 ± 0.002	44.3 ± 2	569

(a) Cell-free extracts from *E. coli* BL21DE3 cells over-expressing the acetoacetyl-CoA reductases from *C. necator* (AAR<sup>Cn</sup>), *Ca. A. phosphatis* (AAR<sup>CAP</sup>) and the artificial Chimera (AAR<sup>Chimera</sup>). For details about cell-free extracts preparation and rate estimates see section Methods. NAD(P)H concentration was 200 μM and acetoacetyl-CoA concentration was 70 μM. 1 U/mg = 1 μmol\*min<sup>-1</sup> per milligram of cytoplasmic proteins.

(b) Data from Haywood and co-workers. The  $k_{cat}$  were calculated from the reported  $V^{max}$  (2.6 U/mg for NADH, 13 U/mg for NADPH) and the molecular weight of the monomer (23 KDa).



Table 4: Reconciled rates and other relevant parameters obtained during the study of the two steady-states characterized by different levels of oxygen limitation.

	Steady-state 1	Steady-state 2
$q_x$ ( $h^{-1}$ )	$0.1098 \pm 0.0041$	$0.0939 \pm 0.0041$
$q_{O_2}$ (mmol/gCDW/h)	$-4.1004 \pm 0.0174$	$-2.8381 \pm 0.0105$
$q_{CO_2}$ (mmol/gCDW/h)	$4.4285 \pm 0.0183$	$3.1196 \pm 0.0158$
$q_{sucrose}$ (mmol/gCDW/h)	$-0.7906 \pm 0.0155$	$-0.6675 \pm 0.0163$
$q_{acetate}$ (mmol/gCDW/h)	$0.0062 \pm 0.002$	$0.198 \pm 0.0239$
$q_{lactate}$ (mmol/gCDW/h)	$0.0495 \pm 0.006$	$0.0043 \pm 0.0004$
$q_{succinate}$ (mmol/gCDW/h)	$0.0377 \pm 0.005$	$0.0222 \pm 0.004$
$q_{formate}$ (mmol/gCDW/h)	b.d.l.	$0.0736 \pm 0.0079$
$q_{PHB}$ (mmol/gCDW/h)	$0.0023 \pm 0.0001$	$0.0676 \pm 0.0034$
Biomass yield (CmolX/CmolS)	$0.5 \pm 0.022$	$0.505 \pm 0.026$
Biomass yield (gCDW/gS)*	0.406	0.410
electrons from sucrose going to oxygen (%)	43	35
electrons from sucrose going to PHB (%)	0.1	3.8
$Y_{PHB}$ (mgPHB/gS)	0.7	25.5
PHB content (%)	0.2	5.8
PHB titer (g/L)	0.01	0.31

\*For the interconversion between CmolX and gCDW, biomass was considered as a "molecule" with a molecular weight  $M_{wx}=23.184$  gCDW/CmolX.

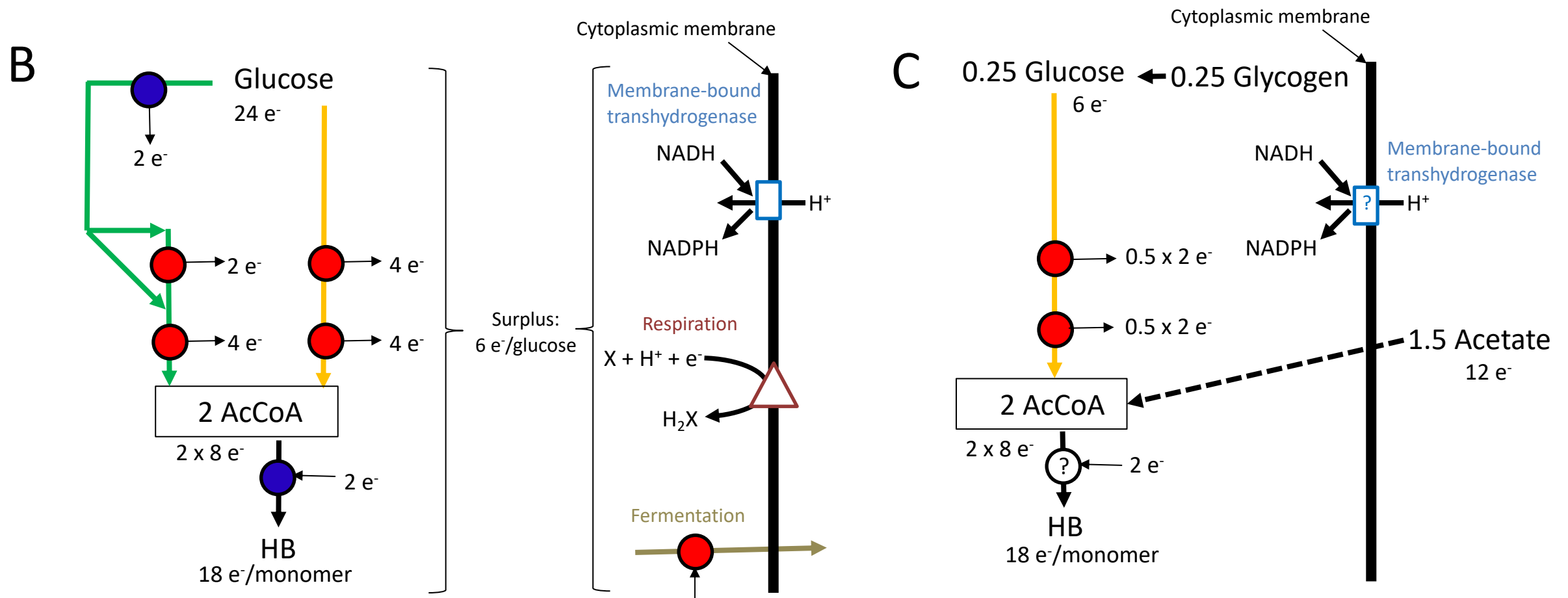
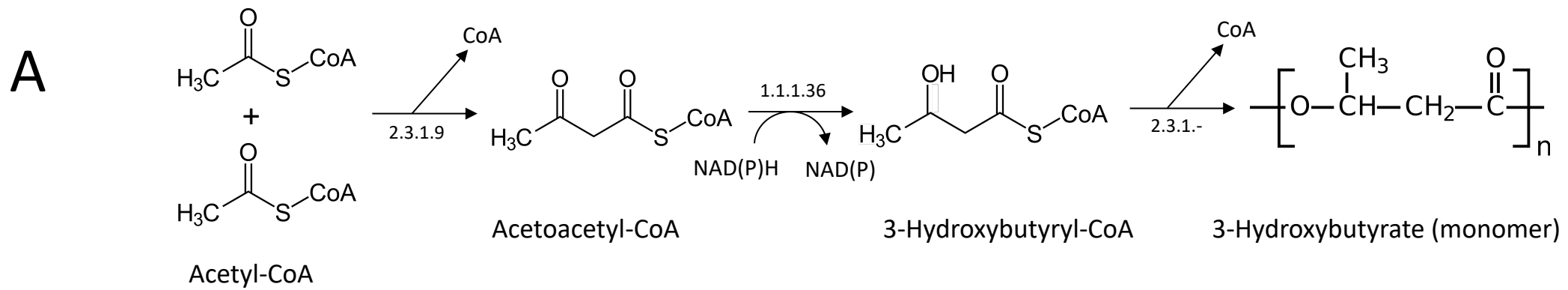
b.d.l.: below detection level.

Figure 1: Electron transfer from carbon source(s) to PHB. NAD(H)-driven processes are represented by red circles and NADP(H)-driven processes by blue circles. **A:** PHB formation pathway. The enzymes catalyzing the steps involved in this conversion are identified using their Enzyme Commission (E.C.) codes. **B:** In the most studied cases—such as recombinant *E. coli* expressing *phaCAB* genes from *C. necator*—glucose is catabolized by Embden–Meyerhof (in orange) or Entner–Doudoroff pathway (in green), yielding two acetyl-CoA (AcCoA) per glucose and eight electrons carried by NADP<sup>+</sup> and/or NAD<sup>+</sup>. One monomer of hydroxybutyrate (HB) contains 18 electrons, and could be form from two acetyl-CoA (16 electrons) and two electrons carried by NADPH. Therefore, there is a surplus of six electrons per glucose that must flow to other electron acceptors (an external acceptor in the case of Respiration, an internally generated acceptor in the case of Fermentation). If glucose oxidation happens only through Embden–Meyerhof pathway, then participation of an energy-dissipating membrane-bound transhydrogenase is also required to transfer electrons from NADH to NADPH. **C:** In the case of *Ca. Accumulibacter phosphatis*, PHB formation takes place under anaerobic conditions. Acetyl-CoA is coming from an internal glycogen reserve and from external acetate, with full electron conservation. Acetate must be taken up and activated to become acetyl-CoA (several steps, represented with a dashed line). The genes encoding for the enzymes catalyzing the reactions of the oxidative branch of pentoses-phosphate pathway or Entner-Doudoroff pathway have not been found in this organism. If PHB accumulation is driven by NADPH, some transhydrogenase mechanism would be required. However, transhydrogenase activity has not been definitively confirmed. If PHB accumulation is driven by NADH, then NADH generated in the lower Embden–Meyerhof pathway could be used to drive PHB formation.

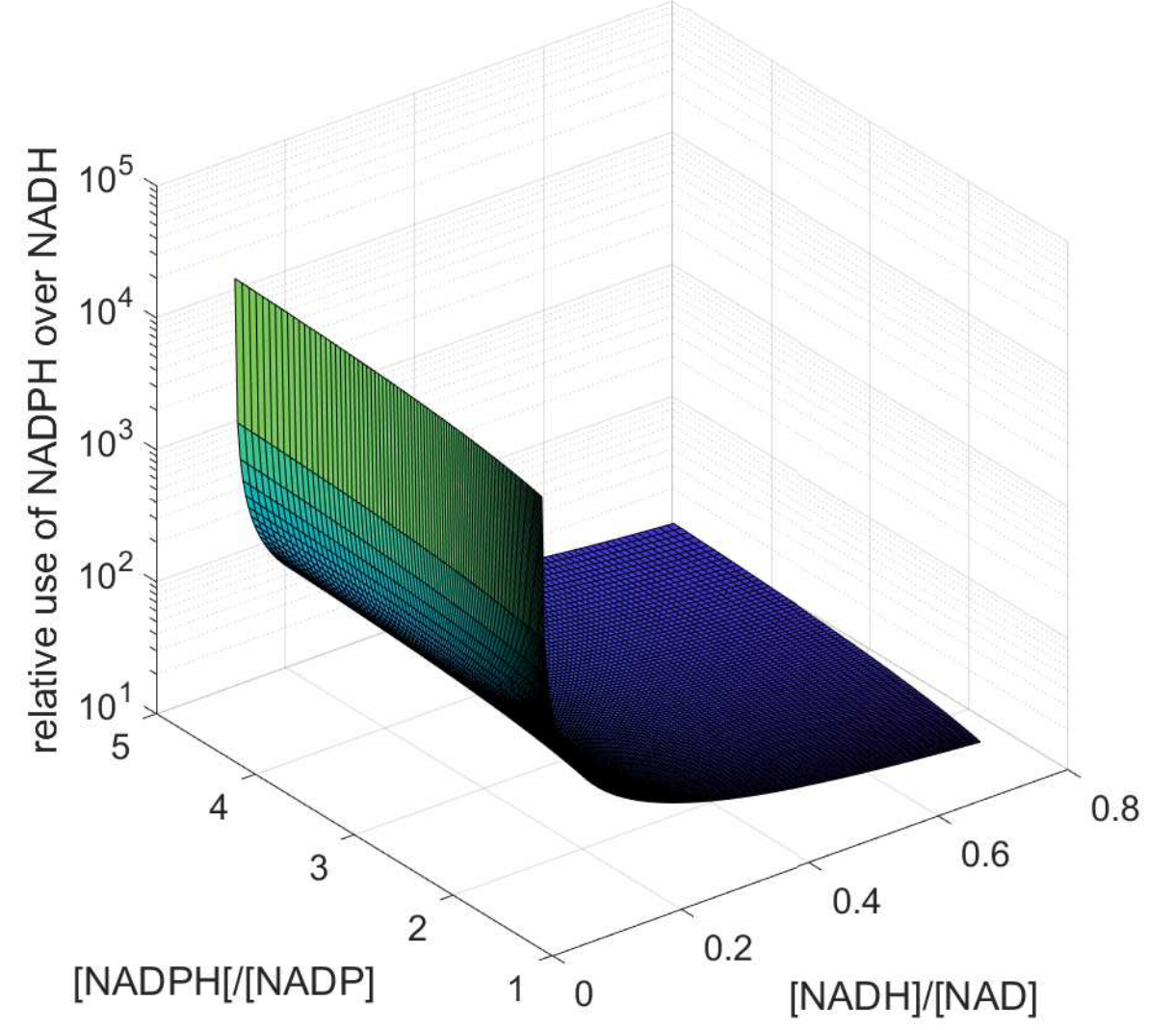
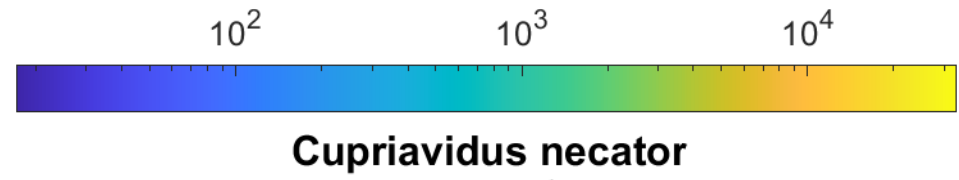
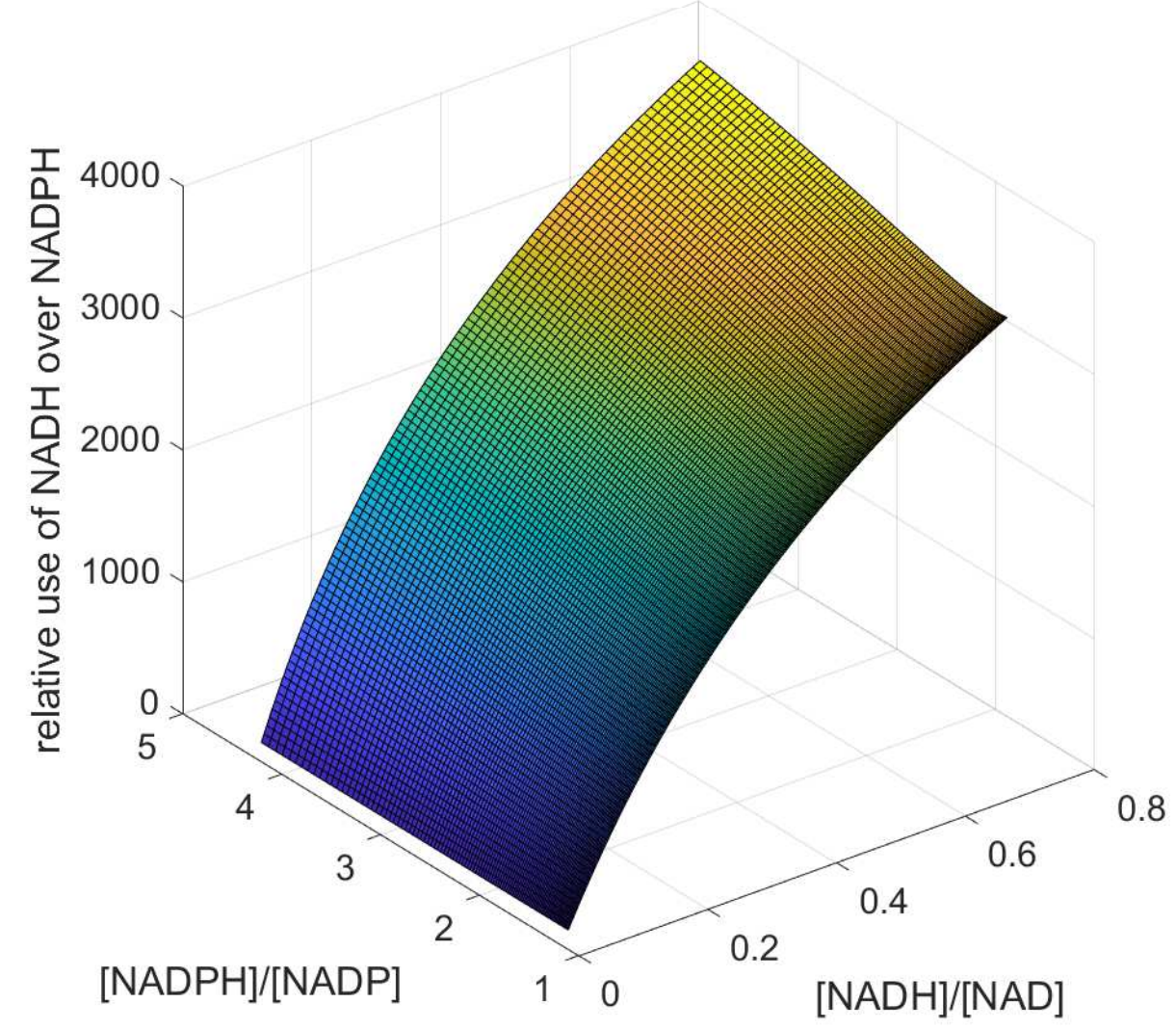
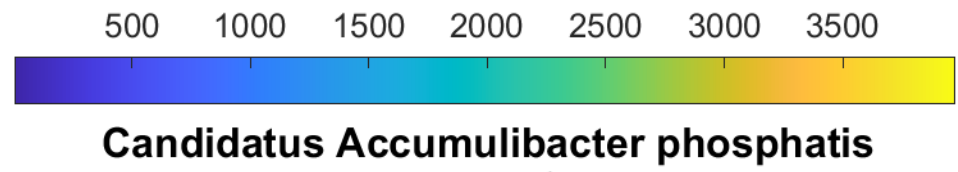
Figure 2: Relative consumption of NADH and NADPH in the reactions catalyzed by the acetoacetyl-CoA reductases from *Ca. A. phosphatis* (left) and *C. necator* (right). The input concentration ranges were  $\text{NAD}^+$ : from 147 to 143  $\mu\text{M}$ , NADH: from 3 to 7  $\mu\text{M}$ ,  $\text{NADP}^+$ : from 50 to 6  $\mu\text{M}$  and NADPH: from 50 to 94  $\mu\text{M}$ .

Figure 3: Involvement of residues of the  $\beta_2\alpha_2$  loop in the cofactor preference. In B and C, labels indicate homologous residues in the homology models (above) and the templates (below, italics). **A:** The superposition of subunits C and D of the homology model of the acetoacetyl-CoA reductase from *Ca. A. phosphatis* in complex with  $\text{NAD}^+$ , shows low conformational variability between subunits. **B:** Superposition of subunit D with subunit D of the acetoacetyl-CoA reductase from *B. cenocepacia* (PDB 4K6F, colored in orange), in complex with  $\text{NADP}^+$ . **C:** Superposition of subunit D of the acetoacetyl-CoA reductase from *Ca. A. phosphatis* with subunit A of the acetoacetyl-CoA reductase from *C. necator* (PDB 4N5N, colored in pink), in complex with  $\text{NADP}^+$ . B and C illustrate the steric hindrance of the voluminous F38 with the 2'-phosphate of  $\text{NADP}^+$ , as well as the impossibility of the positively charged K40 in the acetoacetyl-CoA reductase from *Ca. A. phosphatis* to establish a salt bridge with the 2'-phosphate of the  $\text{NADP}^+$ , as R40 in the acetoacetyl-CoA reductase from *C. necator* does.

Figure

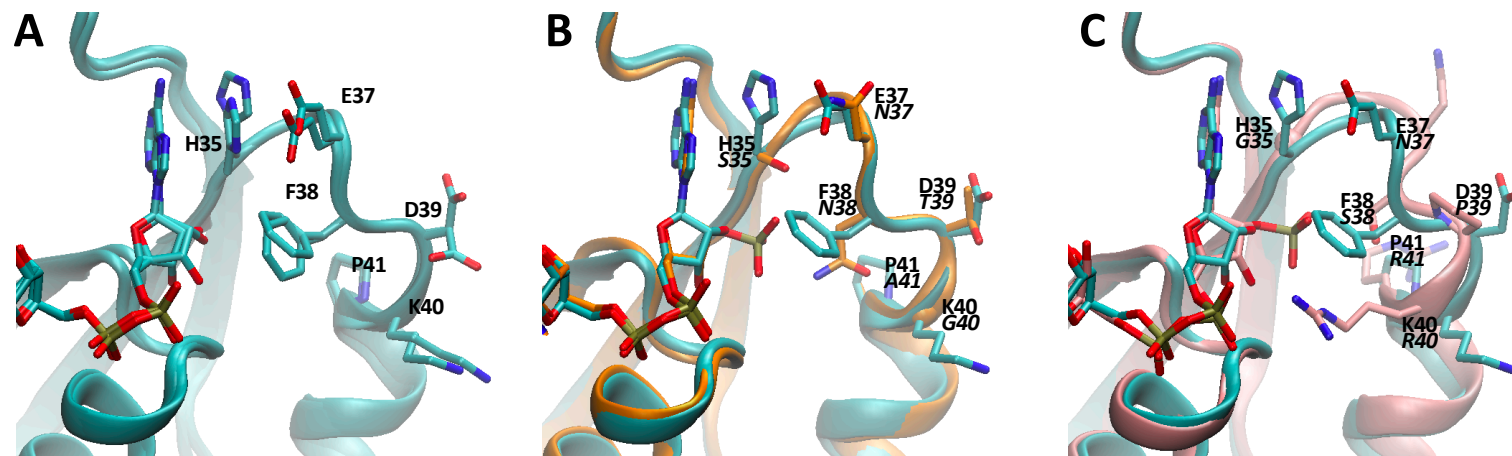


Figure





Figure



**Supplementary File**

[Click here to download Supplementary File: Supplementary materials rebuttal.doc](#)

**Data in Brief**

[Click here to download Data in Brief: Data in Brief Olavarria et al.zip](#)

**Declaration of interests**

The authors declare that they have no known competing financial interests or personal relationships that could have appeared to influence the work reported in this paper.

The authors declare the following financial interests/personal relationships which may be considered as potential competing interests:

## CRedit (Contributor Roles Taxonomy) author Statement

Karel Olavarria: Conceptualization, Methodology, Software, Validation, Formal analysis, Investigation, Data Curation, Writing - Original Draft, Writing - Review & Editing, Visualization, Supervision, Funding acquisition

Alexandre Carnet: Validation, Formal analysis, Investigation, Data Curation, Writing - Review & Editing

Joachim van Ranselaar: Methodology, Formal analysis, Investigation

Caspar Quakkelaar: Formal analysis, Investigation, Data Curation

Ricardo Cabrera: Methodology, Resources, Writing - Review & Editing

Leonor Guedes da Silva: Validation, Investigation

Aron L. Smids: Formal analysis, Investigation, Data Curation

Pablo Villalobos: Methodology, Software

Mark C.M van Loosdrecht: Conceptualization, Resources, Funding acquisition

S. Aljoscha Wahl: Conceptualization, Methodology, Software, Resources, Writing - Review & Editing, Supervision, Project administration, Funding acquisition